Puertes-Castellano, C.; González-Sanchis, MDC.; Lidón, A.; Bautista, I.; Del Campo García, AD.; Lull, C.; Francés, F. (15-0). Improving the modelling and understanding of carbon-nitrogen-water interactions in a semiarid Mediterranean oak forest. Ecological Modelling. 420:1-18. https://doi.org/10.1016/j.ecolmodel.2020.108976

Improving the modelling and understanding of carbon-nitrogen-water interactions in a semiarid Mediterranean oak forest

Cristina Puertes[1], María González-Sanchis[1], Antonio Lidón[1], Inmaculada Bautista[1], Antonio D. del Campo[1], Cristina Lull[1], Félix Francés[1]

[1]Research Institute of Water and Environmental Engineering (IIAMA), Universitat Politècnica de València, Camino de Vera s/n, E-46022 Valencia, Spain

Corresponding author: Cristina Puertes (cripueca@cam.upv.es, +34 963877000 ext. 76152)

Highlights

It is important to include carbon measurements in the calibration process

The nitrogen plant uptake of additional species may be significant

A fixed annual potential uptake may not be appropriate due to seasonality

TETIS-CN is an acceptable tool to reproduce the hydrology and biogeochemistry

Abstract

Mediterranean drylands are often nutrient poor, but parameter requirements of forest ecosystem models are usually high. Therefore, there is a need for developing parsimonious nutrients models. In that sense, this study aims to contribute to a better understanding and modelling of the hydrological and biogeochemical (carbon and nitrogen) cycles and their interactions in semiarid conditions and to test the capability of a new parsimonious model to satisfactorily reproduce them. The proposed model (TETIS-CN) and two additional widely used models were implemented in a *Quercus ilex* forest, and no noteworthy differences were found. Results suggest that: (1) it is important to include carbon observations in the calibration process and to consider all the existing vegetation species in the simulation; (2) a fixed daily potential uptake may not be appropriate to reproduce plant nitrogen uptake; and (3) TETIS-CN, with a lower number of parameters, proved an acceptable tool.

Keywords

Carbon; Nitrogen; Water; Plant-soil interactions; Mediterranean drylands; Quercus ilex

1 Introduction

Precipitation and temperature are the main drivers of ecosystem structure and function, controlling forest stand structure, ecosystem distribution patterns and net primary production at a continental scale (Newman et al., 2006). However, at smaller geographic scales, nutrient availability becomes a limiting factor in many ecosystems (Lozano-García et al., 2016; Newman et al., 2006) and, consequently, ecosystem structure and function usually change along a topographical soil properties gradient (Tateno et al., 2017).

Soils in Mediterranean drylands, are often nutrient poor and, as water content is highly variable, nutrient availability is a frequent limiting factor for their ecosystem development (Sardans and Rodà, 2004). In fact, as net primary production responds to water and nutrient addition (Lü et al., 2018; Sardans and Peñuelas, 2013), in semiarid ecosystems it is difficult to know if vegetation growth is controlled by water, nutrient availability or both (Botter et al., 2008). For this reason, models including nutrient cycling are useful tools which allow the analysis of the relationships and behaviour of these ecosystems (Landsberg, 2003), especially in these Mediterranean ecosystems, which stand out in climate change projections as areas where warmer and drier conditions are predicted, leading to more severe and recurrent droughts (Spinoni et al., 2018). Since most of the annual nutrient requirements are supplied from the decomposition of soil organic matter (Aponte et al., 2010) and plant competition increases in resource-limited environments (Calama et al., 2019), changes in forest ecosystem function are expected because of alterations in water, carbon and nitrogen cycles (Dong et al., 2019). Nevertheless, there is a need to develop and test simple nutrient models (Blanco et al., 2005; Zhang et al., 2013).

Nitrogen is one of these limiting nutrients in Mediterranean ecosystems, for both photosynthetic capacity and growth (Sardans et al., 2008; Uscola et al., 2017) and, consequently, a better knowledge of its storage and cycling is crucial. However, nitrogen availability is markedly linked to the microbial activity because mineral nitrogen is the result of the microbial decomposition of organic matter, which is also influenced by the C:N ratio of this organic matter (Gleeson et al., 2016; Lucas-Borja et al., 2019; Pastor and Post, 1986). Hence, the carbon and nitrogen cycles are inextricably intertwined, which means that nitrogen models should also include the carbon cycle for a proper modelling. Additionally, soil water content and temperature are the main environmental factors influencing these biogeochemical cycles (Manzoni et al., 2004; Rodrigo et al., 1997), especially in water-limited ecosystems (Wang et al., 2017), where significant interactions between microorganisms and water availability exist (Porporato et al., 2015). A clear example are the wetting and drying cycles, a common characteristic in arid and semiarid climates. This process leads to a fast rewetting in the short term after precipitation stimulating microbial activity, which speeds up decomposition and, as a result, nutrient release (Lado-Monserrat et al., 2014). Thus, daily resolution models with a combined analysis of the water, carbon and nitrogen cycles are necessary for the complete understanding of these terrestrial ecosystems (D'Odorico et al., 2004).

Hence, in this article, a new parsimonious model and two existing models of different conceptualization, complexity and purpose, which include the water, carbon and nitrogen cycles, were calibrated using the experimental data recorded in a *Quercus ilex* (holm oak) experimental site under a semiarid climate. The first model is the physically-based model BIOME-BGCMuSo v5.0 (Hidy et al., 2016), which is the modified version of the well-known BIOME-BGC model (Thornton et al., 2002), widely used in natural ecosystems, with an accurate description of the water, carbon and nitrogen cycles and vegetation growth (Chen and Xiao, 2019; Chiesi et al., 2007; Fontes et al., 2010). The second one is the LEACHM model (Hutson, 2003) which is a process-based model developed to simulate water and solute transport in unsaturated or partially saturated

agricultural soils and broadly used in agriculture to simulate the nitrogen cycle (Asada et al., 2013; Jung et al., 2010; Wöhling et al., 2013). These two models have been chosen because both include the groundwater transpiration process, necessary in this case study, and particularly, because BIOME-BGCMuSo v5.0 is able to accurately represent tree responses to environmental conditions and LEACHM has an accurate description of soil hydrological and biogeochemical processes. However, these models have high parameter requirements, and consequently it can be challenging to use them in most situations, mainly because the available information is usually limited. Therefore, the third model is a new parsimonious carbon and nitrogen sub-model which has been coupled to the existing conceptual eco-hydrological model TETIS (Pasquato et al., 2015; Ruiz-Pérez et al., 2016) and named TETIS-CN. Parameter requirements of forest ecosystems models, which commonly include nutrient cycles, is usually high (Härkönen et al., 2019), leading to a cumbersome calibration and frequently, to high computational time due to their complex structure (Jin et al., 2016). Consequently, there is a need of developing parsimonious models under the principle that everything should be made as simple as possible, but not simpler (Stocker et al., 2016).

Within this framework, this study aims to contribute to a better understanding and modelling of the hydrological and biogeochemical (carbon and nitrogen) cycles and their interactions within the soil-plant continuum in semiarid conditions, and also to test the capability of TETIS-CN to satisfactorily reproduce them.

2 Material and methods

2.1 Study area

The study area (Fig. 1) is an experimental fenced plot covering 1800 m^2 located in the public forest *La Hunde*, in east Spain (39°04'29-30'' N, 1°14'25-26'' W elevation 1,080-1,100 m a.s.l.). The slope of the plot is 31% with NW aspect. Soil in this area is loamy textured with a basic pH, high volumetric content of stones, high calcium carbonate content and a decreasing in depth content of soil organic carbon (Table 1). Soil thickness

ranges from 10 to 40 cm, and the parent rock is a karstified Jurassic limestone with numerous fissures, which were revealed by the boreholes (up to 4 m depth) that were drilled along the plot (del Campo et al., 2019b). The water table was not found within this depth, but the parent rock becomes a significant reservoir of deep water (del Campo et al., 2019b) forming a perched aquifer, very common in Mediterranean catchments (Medici et al., 2008). According to a close meteorological station (1960-2011), mean annual precipitation is 466 mm, mean annual temperature is 12.8 °C and mean Hargreaves reference evapotranspiration is 1200 mm. The climate is classified as semiarid according to the Köppen climate classification. The forest is a high density coppice stand of *Quercus ilex* (holm oak) with scarce presence of other species (*Pinus halepensis, Quercus faginea, Juniperus phoenicea and J. oxycedrus*). In May 2012, the forest structure was characterized. Diameter at basal and breast heights were 10.7 cm and 7.7 cm respectively, basal area was 5.6 $m^2\,ha^{-1}$, tree density was 1059/1133 trees ha^{-1} (holm oak/all trees) and the averaged Leaf Area Index (LAI), which was seasonally measured, was 1.13 ± 0.22 $m^2\,m^{-2}$ (2012-2016).

Layer	Stoniness (%)	pH	$CaCO_3$ (%)	SOC (g kg^{-1})	Texture
L Layer	48.4±10.7				
H Layer	59.2±7.1	7.84±0.09	15.3±5.6	131.2±32.0	
0-10 cm	63.9±8.5	8.05±0.11	21.1±6.7	73.2±17.4	44;33;23
10-30 cm	58.6±7.3	8.25±0.12	34.1±6.2	42.3±21.4	57;23;20
30-40 cm	55.5±7.2	8.34±0.04	36.7±1.7	25.1±6.4	48;32;19

Table 1 Soil characteristics of the study site. SOC means soil organic carbon. Soil particle fractions in the following order: sand, silt and clay (%). (Bautista et al., 2015; del Campo et al., 2018).

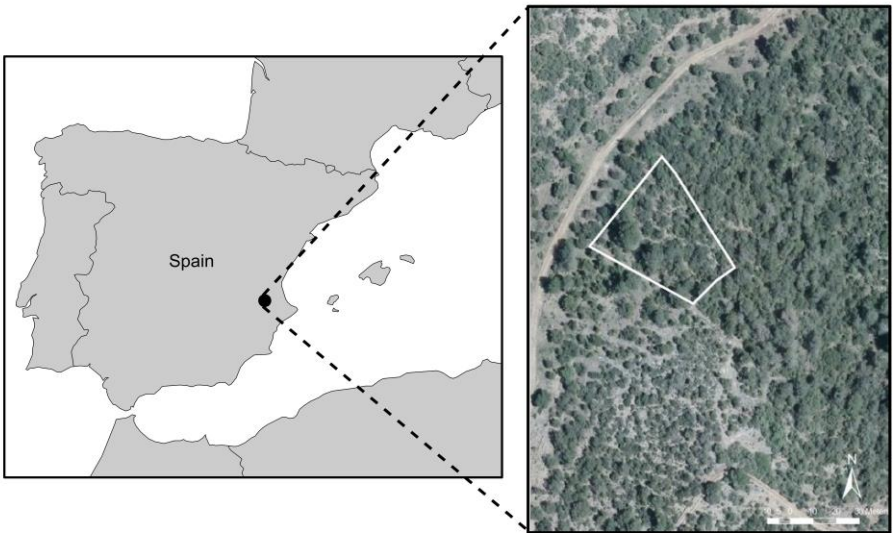

Figure 1 Location of the experimental plot study site.

2.2 Environmental variables and hydrological field measurements

By means of a central data-logging unit and different instruments connected to it, data were registered and stored during the observational period, from 01/10/2012 to 26/04/2016. The data-logger was programmed to record all meteorological data and field measurements every 10 minutes and averaged on a daily basis. Table 2 shows a summary of the data, while a complete description of the instrumentation and methodology employed to obtain the data can be found in del Campo et al. (2019a, 2018).

Data	Sensor	Type	Temporal resolution
Precipitation	Davis tipping bucket	Input	Continuously
Air temperature	Decagon Devices T/RH sensor	Input	Every ten minutes
Relative humidity	Decagon Devices T/RH sensor	Input	Every ten minutes
Throughfall	del Campo et al. (2018)	Input	Every ten minutes
Runoff	Diehl Metering Altair v4 volumetric counters	State variable	Every ten minutes
Soil water content	15 FDR probes (EC-5, Decagon Device)	State variable	Every ten minutes
Transpiration	ICT international sap flow sensor	State variable	Every thirty minutes
Field LAI	LAI-2000 sensor	Input	Seasonally
Satellite LAI	Level-4 MODIS global LAI satellite product (NASA, LPDAAC)	Input	Weekly
Mineralization	Resin core method (DiStefano and Gholz, 1986)	State variable	Every two months
Nitrification	Resin core method (DiStefano and Gholz, 1986)	State variable	Every two months

Nitrogen leaching	Resin core method (DiStefano and Gholz, 1986)	State variable	Every two months
NH_4^+ soil content	Flow injection analyser (FIAStar 5000, Foss Tecator, Höganäs, Sweden)	State variable	Every two months
NO_3^- soil content	Flow injection analyser (FIAStar 5000, Foss Tecator, Höganäs, Sweden)	State variable	Every two months
Soil respiration	EGM-4 environmental gas monitor from PP System Company	State variable	Every one or two months

Table 2 Data, sensor employed to record it, type of data and temporal resolution.

A Davis tipping bucket rain gauge placed in an open area 20 m away from the plot was used to continuously measure precipitation, and by means of a Decagon Devices T/RH sensor placed inside the plot at 2 m height above ground surface, air temperature and relative humidity were recorded. Throughfall was measured according to the methodology described in del Campo et al. (2018).

Soil water content was measured by means of 15 FDR probes (EC-5, Decagon Device) installed at 5, 15 and 30 cm depth and the default calibration for mineral soils was used. At the lower boundary of the slope, runoff was measured in two collecting trenches by means of Diehl Metering Altair v4 volumetric counters.

In order to estimate stand transpiration, sap flow velocity was measured through the Heat Ratio Method (Burgess et al., 2001) in 14 trees, which were divided into 4 different diametrical classes. One ICT international sap flow sensor was installed in each tree on the north trunk side at 0.3 - 1.0 m height. These sap flow measurements were upscaled to stand transpiration accounting for the density of trees and their diameter frequency distribution.

It is worth noting that the impairment between soil water content and transpiration measurements during the summer months (i.e. transpiration > measured soil water content changes) suggests that *Q. ilex* has access to subsoil water resources (del Campo et al., 2019a) and thus, additional groundwater transpiration is considered in this study (Puertes et al., 2019).

LAI was seasonally measured in the field 12 times during the observational period by means of a LAI-2000 sensor, and in order to extend the data series, the estimations from the level-4 MODIS global LEAF Area Index satellite product (NASA, LPDAAC) were used (del Campo et al., 2019a; Puertes et al., 2019).

2.3 Carbon and nitrogen field measurements

In the case of the carbon and nitrogen field measurements, the observational period only covers the first two hydrological years (01/10/2012 – 30/09/2014). Soil samples were collected from the first 15 cm of soil every two months approximately, and from 9 different sites homogenously distributed inside the plot in order to deal with the common heterogeneity in the spatial distribution of carbon and nitrogen, which is mainly caused by the patchy distribution of vegetation and its variability in life forms (Austin et al., 2004). Mineralization, nitrification and leaching were measured using the resin core method (DiStefano and Gholz, 1986). Soil samples were placed in PVC tubes with resin traps, where they were left incubating (in situ buried cores). Part of the same soil used to fill the tubes was kept refrigerated and transported to the lab where the initial ammonium (NH_4^+-N) and nitrate (NO_3^--N) soil contents were obtained by means of a flow injection analyzer (FIAStar 5000, Foss Tecator, Höganäs, Sweden). The process was repeated approximately every two months, replacing the incubated soil by new soil, and taking it and a sample of the new soil to the lab, where initial (new soil) and final (incubated soil) NH_4^+-N and NO_3^--N soil contents were obtained. From the mass balance between the initial and final NH_4^+-N and NO_3^--N soil contents, net mineralization and net nitrification accumulated during the incubation period were calculated. The NH_4^+-N and NO_3^--N accumulated in the deeper resin trap corresponded to the NH_4^+-N and NO_3^--N accumulated leaching, whilst the initial NH_4^+-N and NO_3^--N soil contents corresponded to the punctual NH_4^+-N and NO_3^--N observations.

An EGM-4 environmental gas monitor from PP System Company was used to obtain the CO_2 efflux (total soil respiration). All the measurements were made at midday, between

1100 and 1300 CET and every one or two months on 9 PVC collars (10 cm in diameter and 5 cm depth) introduced 3 cm into the soil.

2.4 Models description

The models used in this study are described in the following lines. BIOME-BGCMuSo and LEACHM are briefly described, while TETIS-CN is described in detail, as it has been developed during this study. Table 3 shows a comparison between model characteristics.

	BIOME	LEACHM	TETIS-CN
Hydrological parameters	-	15 + 9 nlayers	21
Carbon and nitrogen parameters	-	19 + 5 nlayers	19
Total number of parameters	194	34 + 14 nlayers	40
Number of layers	10	n (8 herein)	2
Soil water movement	Tipping bucket water balance	Richards' equation	Tipping bucket water balance (4 tanks)
Transpiration	Based on the Penman–Monteith equation using stomatal conductance	Nimah and Hanks (1973)	Multiplicative function relating transpiration and the environmental variables
Dead plant material fractions	5	1	1
Soil organic matter fractions	4	2	2
Inorganic nitrogen fractions	2	2	2
Soil organic matter decomposition	First-order kinetics	First-order kinetics	First-order kinetics
Nitrogen transformations	First-order kinetics	First-order kinetics	First-order kinetics
Nitrogen sorption	Fixed percentage	Linear isotherm	Linear isotherm
Solute movement	Advective movement	Convection-diffusion equation	Advective movement

Table 3 Models characteristics comparison.

2.4.1 BIOME-BGCMuSo model

The BIOME-BGCMuSo v.5.0 model (Hidy et al., 2016) is the modified version of BIOME-BGC model (Thornton et al., 2002), hereafter referred as BIOME, which has been widely used in natural ecosystems (Chen and Xiao, 2019; Chiesi et al., 2007; Fontes et al., 2010). It is a biogeochemical model with multilayer soil sub-model, which simulates the storage and flux of water, carbon, and nitrogen between the ecosystem and the

197 atmosphere, and within the components of the terrestrial ecosystem. It uses a scale of 1
198 m^2, daily meteorological data, site-specific data, ecophysiological data, carbon-dioxide
199 concentration (CO_2) and N-deposition data to simulate the biogeochemical processes of
200 the given biome. The soil profile is divided into 10 layers and the main simulated
201 processes assessed are photosynthesis, allocation, litterfall, carbon, nitrogen and water
202 dynamics in the plant, litter and soil. The model is composed by 60 plant functioning
203 parameters, 24 senescence and soil parameters, 12 growing season parameters, 14 rate
204 scalars, 7 CH4 parameters and 7 phenological phases, with 11 parameters each (Table
205 A.1).
206 As stated by Hidy et al. (2016), the three most important blocks of the model are the
207 phenological, the carbon flux, and the soil flux block. The phenological block calculates
208 foliage development and therefore affects the accumulation of carbon and nitrogen in
209 leaf, stem (if present), root and consequently the amount of litterfall. In the carbon flux
210 block, gross primary production (GPP) of the biome is calculated using Farquhar's
211 photosynthesis routine (Farquhar et al., 1980) and the enzyme kinetics model based on
212 Woodrow and Berry (1988). Autotrophic respiration is separated into maintenance and
213 growth respirations. In addition to temperature, maintenance respiration is calculated as
214 the function of the nitrogen content of living plant pools, while growth respiration is a fixed
215 proportion of the daily GPP. The soil block describes the decomposition of dead plant
216 material and soil organic matter, nitrogen mineralization and nitrogen balance (Running
217 and Gower, 1991). Dead plant material is partitioned into coarse woody debris and litter,
218 the latter represented by 4 different fractions. Soil organic matter is also divided into four
219 fractions: fast, medium, slow and recalcitrant (humus). Two elements (carbon and
220 nitrogen) represent each fraction and both elements in litter and soil organic matter are
221 transferred into sequentially slower decomposing pools. Organic carbon decomposition
222 is calculated by multiplying the decomposition rate by the carbon content in each pool
223 (i.e. first-order kinetics). Heterotrophic respiration is calculated through the respiration
224 fraction, which is different for each pool. All rates are adjusted based on temperature and

soil water content. The soil hydrological calculation can be carried out by using Richards's equation or a "tipping bucket" water balance approach (used in this case study). The model differentiates between soil and groundwater transpiration.

2.4.2 LEACHM model

The second model employed in this study is the LEACHM model (Hutson, 2003). LEACHM has been broadly used for simulating water and solutes movement in unsaturated soils, mainly in agricultural soils (Asada et al., 2015, 2013; Contreras et al., 2009; Lidón et al., 2013; Nasri et al., 2015). It is a one-dimensional model that divides the soil profile into a user's fixed number of horizontal layers of equal thickness. It employs finite differencing approximation techniques to simulate flow and redistribution of water and solutes; the model homogenously divides the time step and inputs at least into 10-time intervals per day. Its hydrological sub-model is composed of 24 parameters, nine of them defined for each soil layer, and its carbon-nitrogen sub-model is also composed of 24 parameters (Table A.2), five of them defined for each soil layer. Therefore, the model is composed of 48 parameters, but 14 of these parameters are defined for each soil layer, and consequently, increasing the number of layers highly increases the number of parameters to be estimated or calibrated.

In order to describe the water flow in the unsaturated zone, LEACHM uses the Richards' equation, in which soil moisture and hydraulic conductivity are related by the equation proposed by Campbell (1974). Runoff estimate is based on the equation proposed by Williams (1991), with the advantage of adjusting the runoff curve number according to the slope. Potential evapotranspiration is split into potential evaporation and potential transpiration according to the plant cover fraction. Actual evaporation is calculated as a function of the potential evaporation and the maximum possible evaporative flux density while actual transpiration is calculated following Nimah and Hanks (1973) as a function of the soil's unsaturated hydraulic properties and the effective water potential gradient at roots-soil interface.

Soil organic matter is divided in LEACHM into three different fractions: plant residue (litter), manure (easily degradable) and humus (relatively stable), each one with its corresponding two pools (carbon and nitrogen). Biomass remains an integral part of the plant residue pool. Soil organic matter decomposition is described by first-order kinetics in the carbon pools and nitrogen transformations are given by the C/N ratio of the decomposition products, that in turn, controls net mineralization, that is, the mineral nitrogen released or consumed by the microbial biomass. The synthesis efficiency factor defines the relative production of CO_2 (heterotrophic respiration) and humus, while the humification factor determines the split between humus and biomass. Nitrification, volatilization, and denitrification processes are also modelled by first-order kinetics. Ammonium adsorption and desorption by clay colloids is modelled by a linear sorption isotherm. All transformation equations are corrected accounting for the influence of soil water content and soil temperature (Q_{10} type function), however, it should be highlighted that an error was found in the code, by which, the temperature correction function was not changing the daily temperature in the case of using the Richards' equation. This error was corrected. Solute transport is modelled following the convection-diffusion equation. Finally, plant nitrogen uptake occurs in the transpiration flux, but if this does not satisfy the requirements (daily potential uptake), a diffusive component for nitrate is considered. In the case of perennial vegetation, a constant daily potential uptake is calculated from the yearly value.

Additionally, in this case study, as LEACHM does not simulate plant growth, two new parameters were added to the model with the aim of characterize the plant residue input: a plant death constant (gC m^{-2} day^{-1}), which accounts for litterfall and root mortality, and the C/N ratio of the plant residue. Since the rate of added organic matter changes over time, a fixed annual curve based on the measured litterfall curve was considered.

2.4.3 TETIS-CN model

The TETIS-CN model divides the soil profile into two layers, allows fixing an evaporation depth in this shallow first layer and hence, the evapotranspiration split between bare soil evaporation and transpiration in this first layer, which is necessary in order to properly reproduce nutrient cycles. On the one hand the hydrological sub-model (Pasquato et al., 2015; Ruiz-Pérez et al., 2016) is based on a tank type conceptualization in which water moves downwards as long as the tank outflow capacity is not exceeded (Fig. 2) and is composed of 25 parameters. On the other hand, the new carbon and nitrogen sub-model (Fig. 3) is based on the model proposed by Porporato et al. (2003) because it is already a parsimonious model. It divides soil organic matter into three fractions, which is in good agreement with Batlle-Aguilar et al. (2011) and Jenkinson et al. (1990), who proposed that models should divide soil organic matter at least between two and four fractions to obtain reliable results, while more complex models commonly comprise five (Lardy et al., 2011) or even more, as BIOME. However, this model has been improved, mainly to adapt it to semiarid climates, where temperature and soil water content are the main environmental drivers (Manzoni et al., 2004). Volatilization, denitrification, NH_4^+ sorption and a temperature correction function have been included, and additionally, the soil water correction functions have been improved. Hence, this final carbon-nitrogen sub-model is composed of 19 parameters (Table A.3), leading to a total of 44 parameters and in order to explore the basic mechanisms of the carbon and nitrogen cycles, TETIS-CN was used as simple as possible, keeping its dynamic vegetation sub-model deactivated and introducing as inputs the LAI values simulated by the dynamic vegetation sub-model.

The first tank (T1) represents the interception process. Water is stored in this tank depending on its storage capacity and it can only exit by direct evaporation. The next two tanks (T2 and T3) represent the soil static storage. From the shallow layer, water can exit by bare soil evaporation and superficial roots transpiration, while from the underlying layer only transpiration is considered. Tanks T4 and T5 represent the runoff

generation, which act as linear storages characterized by residence times. Lastly, as in this case *Q. ilex* has access to subsoil water resources, the modification introduced by Puertes et al. (2019) in order to consider groundwater transpiration in this experimental plot, was used. The modification consists in the introduction of an intermediate tank (T_6) between the soil and the aquifer from which groundwater transpiration is calculated. Transpiration and evaporation are calculated using the reference evapotranspiration. Transpiration is corrected by a water stress factor, the vegetation's LAI, the vegetation cover fraction and the percentage of roots in each layer, while evaporation is only corrected by a water stress factor and the vegetation cover factor.

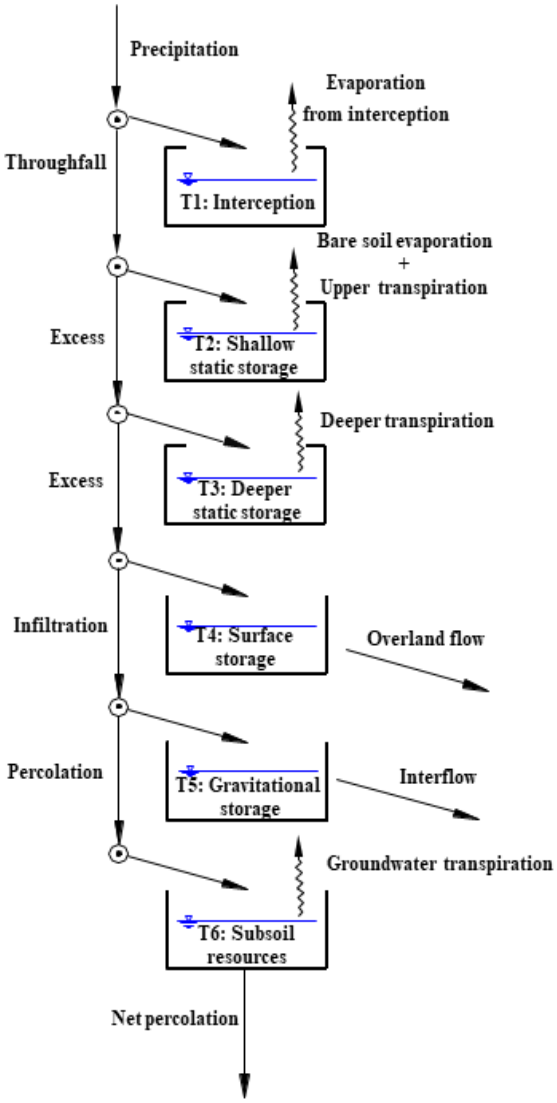

Figure 2 Schema of the adapted TETIS-CN hydrological sub-model to the case study.

316 Soil organic matter is divided into three fractions: litter, humus and biomass; each one
317 represented by two pools (carbon and nitrogen). The mass balance between these pools
318 is calculated in carbon terms and it is transformed to nitrogen by the C/N ratio of each
319 fraction. Microbial death, which is recirculated to the litter pool, is represented by a simple
320 first-order kinetic, without considering soil water content or temperature influence:

321 $$MD = k_{md} C_b \qquad Eq(1)$$

322 where *MD* is microbial death (gC m^{-3} day^{-1}), k_{md} is microbial biomass death rate (day^{-1})
323 and C_b is biomass soil carbon content (gC m^{-3}). However, as soil organic matter
324 decomposition not only relies on the amount of decomposable material but also on the
325 microbial activity, soil organic matter decomposition is described by a multiplicative
326 expression:

327 $$DEC_i = \varphi f(\vartheta) f(t) k_i C_b C_i \qquad Eq(2)$$

328 which is still a first-order kinetics, but it includes the influence of the amount of organic
329 matter and the decomposers (Manzoni and Porporato, 2007). The term φ is a
330 dimensionless factor which has a value of 1, unless the litter is poor in nitrogen and
331 immobilization is not enough for the microorganisms, $f(\vartheta)$ and $f(t)$ are terms accounting
332 for the influence of soil water content and soil temperature, k_i is the decomposition rate
333 of the litter or hummus soil carbon content (m^3 day^{-1} gC^{-1}) and C_i is litter or hummus soil
334 carbon content (gC m^{-3}). Nitrogen net mineralization is controlled by the C/N ratio of the
335 biomass, which should remain constant. The respiration rate defines the relative
336 production of CO_2 (heterotrophic respiration) while the humification factor determines the
337 split between humus and biomass. Nitrification is calculated similarly to decomposition:

338 $$NIT = \varphi f(\vartheta) f(t) k_{nit} C_b {NH_4^+}_d \qquad Eq(3)$$

339 where *NIT* is nitrification (gN m^{-3} day^{-1}), k_{nit} is nitrification rate (m^3 day^{-1} gN^{-1}) and ${NH_4^+}_d$
340 is the dissolved fraction of NH_4^+-N soil content (gN m^{-3}).

Volatilization and denitrification processes are less important at the daily-to-seasonal time scale in natural soils (Porporato et al., 2003), hence, simple first-order kinetics are used. Volatilization is calculated as:

$$Vol = f(\vartheta)f(t)k_{vol}NH_4^+{}_d \qquad Eq(4)$$

where *Vol* is volatilization (gN m^{-3} day^{-1}) and k_{vol} is volatilization rate (day^{-1}). Denitrification is calculated as:

$$De = f(\vartheta)k_{de}NO_3^- \qquad Eq(5)$$

where *De* is denitrification (gN m^{-3} day^{-1}), k_{de} is denitrification rate (day^{-1}) and NO_3^- is NO_3^--N soil content (gN m^{-3}). NH_4^+ adsorption and desorption by clay colloids is modelled in the simplest way, by a linear sorption isotherm:

$$c_s = k_d c_L \qquad Eq(6)$$

where k_d is NH_4^+ distribution coefficient (dm^3 kg^{-1}), c_s is NH_4^+-N concentration in the sorbed phase (mgN kg^{-1}) and c_L is NH_4^+-N concentration in solution (mgN dm^{-3}).

Nitrogen uptake by vegetation is considered to occur proportionally to the transpiration flux, and if the nitrogen potential uptake is not accomplished, a diffusive flux is triggered, which is proportional to the nitrogen content and a diffusion coefficient. A constant daily potential uptake calculated from the yearly value is considered. NH_4^+-N and NO_3^--N leaching is considered to occur proportionally to the percolation flux (i.e. advective movement). In the case of NH_4^+-N, only the dissolved fraction is considered to be available for nitrification, volatilization, plant nitrogen uptake and leaching.

The function controlling the influence of soil water content on decomposition, mineralization and nitrification processes is:

$$f(\vartheta) = \begin{cases} \vartheta/\vartheta_T & \vartheta < \vartheta_T \\ \vartheta_T/\vartheta & \vartheta \geq \vartheta_T \end{cases} \qquad Eq(7)$$

where ϑ is soil moisture (cm cm^{-1}) and ϑ_T a soil moisture threshold (cm cm^{-1}). Instead of field capacity, a threshold is used in order to reproduce the pulse dynamics observed in semiarid environments (Medici et al., 2012). This threshold is included as a parameter in the model. The function controlling the influence of soil water content on volatilization is:

$$f(\vartheta) = \begin{cases} \vartheta/\vartheta_T & \vartheta < \vartheta_T \\ 1 & \vartheta \geq \vartheta_T \end{cases} \quad Eq(8)$$

and the soil water content correction function for denitrification is:

$$f(\vartheta) = \begin{cases} 0 & \vartheta < \vartheta_T \\ 1 & \vartheta \geq \vartheta_T \end{cases} \quad Eq(9)$$

The function controlling the influence of temperature is the one proposed by Kätterer and Andrén (2001).

Finally, as with LEACHM, in order to characterize the plant residue input, a plant death constant (gC m^{-2} day^{-1}) and its C/N ratio were added as parameters and a fixed annual curve, based on the measured litterfall curve, was also considered.

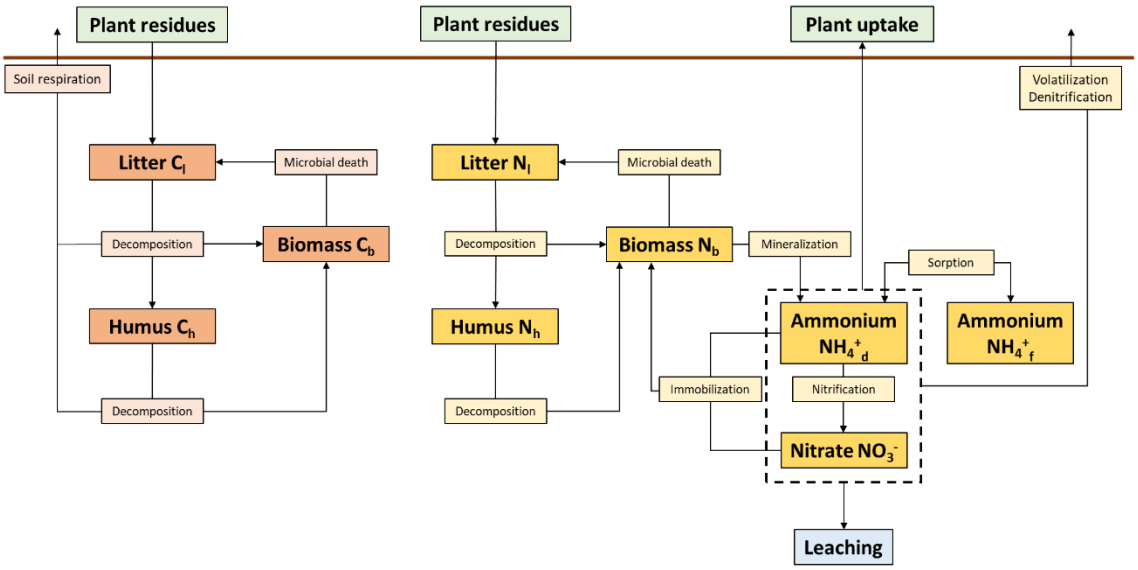

Figure 3 Schema of the TETIS-CN carbon and nitrogen sub-model.

2.5 Model implementation

In order to make precise predictions, obtaining the effective parameters through a calibration process is crucial. As models are a simplified representation of the reality, their parameters will be representative of the modelling scale and different to the ones measured in field (Mertens et al., 2005), being their main purpose to compensate for the model structure errors, the spatial and temporal scale effects and the observational errors (Abbaspour et al., 2007; Francés et al., 2007). Consequently, the three models

were calibrated and validated using some measurements of the observed state variables and only validated using the remaining measurements.

2.5.1 Model evaluation

The simulation period included the period with available observations. In the case of the water cycle, from 01/10/2012 to 26/04/2016, including a previous warming-up period (01/08/2012 to 30/09/2012), in which only meteorological data were available. The first two hydrological years were selected to calibrate the hydrology, and the remaining period to validate it. In the case of the carbon and nitrogen cycles, the available observations were from 01/10/2012 to 30/09/2014. The first year was used to calibrate the models, and the second one was used as validation; therefore, as model performance in terms of biogeochemistry was measured during two hydrologically calibrated years, the errors in reproducing the hydrology were not transmitted to the biogeochemical performance of the models. The hydrology was simulated for all the soil profile, however, due to the nitrogen measurements are representative of the first 15 cm of soil, the biogeochemistry was simulated only in these 15 cm of soil in this case study. BIOME and TETIS-CN were directly used with a daily time-step, while LEACHM was used with a 0.05-day time-step, although the output data are expressed daily. They were calibrated and validated using the field measurements of transpiration, soil water content, NH_4^+-N soil content, NO_3^--N soil content, accumulated net mineralization and accumulated net nitrification. In addition, interception was used in the calibration process in the case of BIOME and TETIS-CN, and the measurements of mineral nitrogen leaching and soil respiration were only used to validate the models.

Soil water content measurements were used daily, but transpiration measurements were averaged on a weekly basis. As LEACHM employs weekly reference evapotranspiration and temperature, although the results are daily, it is expected to simply match the weekly transpiration value. Thus in order to compare the models, all were calibrated using weekly transpiration values. Interception data, in the case of BIOME and TETIS-CN,

were used accumulated for the whole calibration period with the aim of improving the hydrological annual balance representation. LEACHM does not consider the process of interception, being throughfall the required input. Moreover, LEACHM and TETIS-CN do not calculate autotrophic respiration, therefore, in order to compare the results, the total soil respiration measurements were divided into autotrophic and heterotrophic respiration. According to Hanson et al. (2000), heterotrophic respiration in forests averages 51.4% of total soil respiration (sample of 37 forests), therefore, this value was used. Although soil respiration measurements correspond to the whole soil profile, as microbial biomass content is substantially higher in the surface soil layers (Fierer et al., 2003; Taylor et al., 2002), the calculated heterotrophic respiration can be compared with the results of the models, which correspond to the first 15 cm of soil. However, as it is a transformed variable, it was not used in the calibration process.

The performance of the models was measured using the following state variables and goodness-of-fit indices: the Nash and Sutcliffe efficiency index (NS) was used in the case of soil water content (NS_SWC) and transpiration (NS_TR), while the balance error (BE) was used in the case of interception. The Root Mean Squared Error (RMSE) was used to evaluate the performance of the models in terms of NH_4^+-N soil content (RMSE_NH_4^+), NO_3^--N soil content (RMSE_NO_3^-), accumulated net mineralization (RMSE_Min), accumulated net nitrification (RMSE_Nit), accumulated mineral nitrogen leaching (RMSE_Leach) and heterotrophic respiration (RMSE_Resp).

2.5.2 Calibration process

In the case of BIOME, an automated model parameter estimation was conducted using PEST (model-independent parameter estimation program) (Doherty, 2007), which has implemented a variant of the Gauss-Marquardt-Levenberg method of nonlinear parameter estimation. PEST minimizes the weighted sum of squared residuals between observed and predicted values of the selected state variables. However, LEACHM and TETIS-CN were calibrated in two different phases. As these models do not explicitly

consider vegetation growth, vegetation transpiration is not influenced by nitrogen uptake, and consequently, the inclusion of the carbon and nitrogen to the simulation does not affect the hydrological cycle. Hence, the first phase was the hydrological calibration. Initially, a manual calibration was performed and then an automatic calibration was carried out using the Multiobjective Shuffled Complex Evolution Metropolis (MOSCEM) algorithm (Vrugt et al., 2003), based on the concept of Pareto-optimal solutions. The population size was set to 50.000 and the number of complexes to 200. The compromise solution from the Pareto front was chosen according to the criteria: minimum Euclidean distance calculated using NS_SWC and NS_TR and, a BE less than 40% only in the case of TETIS-CN. A more detailed description of this calibration process can be found in Puertes et al. (2019). Thereafter, the carbon and nitrogen sub-models were calibrated. With LEACHM, as the observed data are scarce, the same mineralization, nitrification and denitrification rates were used for all soil layers (15 cm). An initial manual calibration was done, for which the initial parameters values were found in the literature (Jung et al., 2010; Ramos and Carbonell, 1991; Schmied et al., 2000). Previous experience with the model and field observations were also considered. Later, an automatic calibration was carried out using the MOSCEM algorithm (Vrugt et al., 2003) with a population size of 50.000 and 200 complexes. The solution with a smaller value of Euclidean distance, calculated using the RMSE_NH_4^+, RMSE_NO_3^-, RMSE_Min and RMSE_Nit, was chosen from the Pareto front as a compromise solution.

The calibration of the TETIS-CN carbon and nitrogen sub-model was similar. A previous manual calibration was carried out, for which the initial values where found in literature (D'Odorico et al., 2003; Manzoni et al., 2004; Manzoni and Porporato, 2007) and taking into account field observations. Then, the automatic calibration using the MOSCEM algorithm (Vrugt et al., 2003) was carried out. In this case, as TETIS-CN is not as time-demanding as LEACHM, the population size was set to 100.000 and the number of complexes to 250. Likewise, the solution with a smaller value of Euclidean distance,

calculated using the RMSE_NH_4^+, RMSE_NO_3^-, RMSE_Min and RMSE_Nit, was chosen from the Pareto front as a compromise solution.

3 Results

The final parameter values are listed in Table A.1 for BIOME. In the case of LEACHM and TETIS-CN the hydrological parameters are listed in Puertes et al. (2019) and the carbon and nitrogen parameters in Table A.2 and Table A.3 respectively.

In terms of soil water content (Fig. 4 and Fig. 5), during the calibration period BIOME showed a very good performance, while LEACHM and TETIS showed a good performance (Moriasi et al., 2007). Only LEACHM was able to maintain this performance throughout the validation period, TETIS-CN decreased to a satisfactory performance and BIOME to an unsatisfactory performance (Moriasi et al., 2007). Conversely, only BIOME was able to reproduce the low soil water content observed during the warmest and driest months, from June to September approximately. Neither LEACHM nor TETIS-CN were able to reproduce this effect and a significant disagreement between observed and simulated was observed during these months, with a NS index of 0.41 and 0.04 respectively.

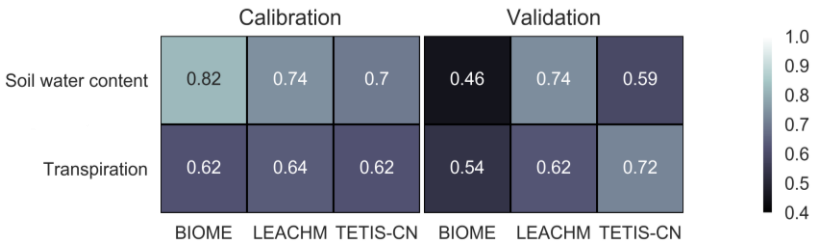

Figure 4 Heatmap representation of soil water content and weekly transpiration NS indices.

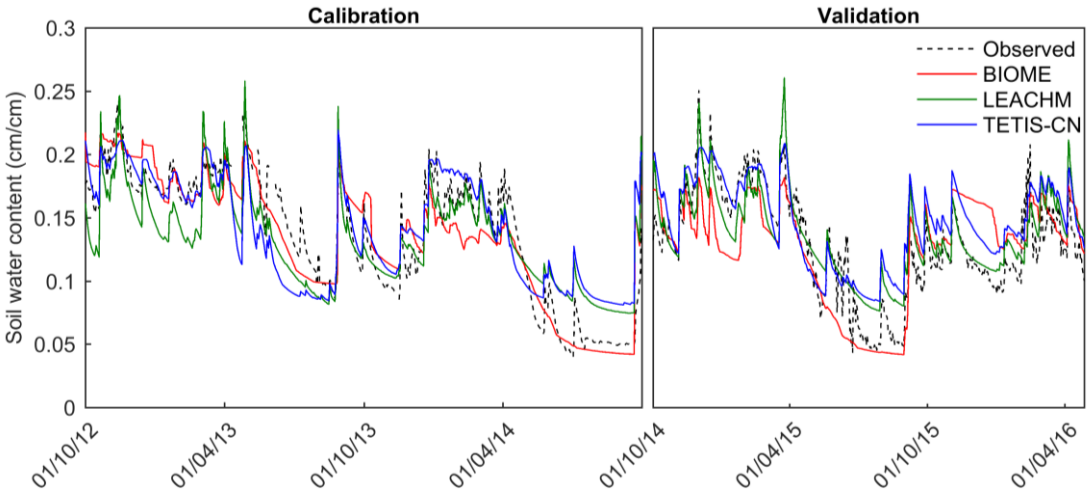

Figure 5 Observed and simulated soil water content

Likewise, the three models reproduced transpiration satisfactorily (Moriasi et al., 2007) during both, calibration and validation periods (Fig. 4 and Fig. 6). Nonetheless, none was able to reproduce transpiration during the warmest months (June – September) and BIOME worsened its performance during the validation period.

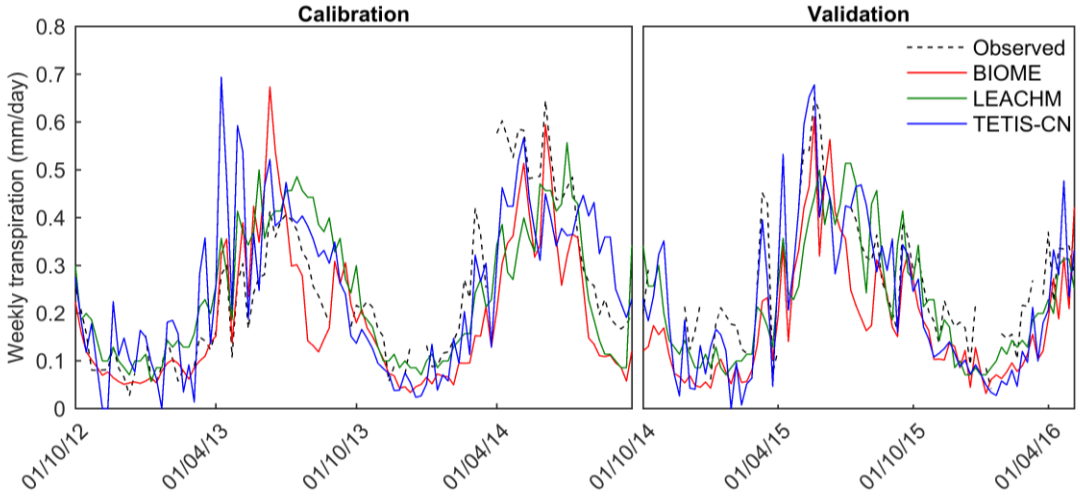

Figure 6 Observed and simulated transpiration

Regarding the water balance (Table 4), some differences were found mainly in the soil evaporation and transpiration results. Both values were lower when using BIOME, which underestimated total transpiration, leading to a higher percolation value. Nevertheless, the main differences were found in the evapotranspiration partitioning results of TETIS-CN, which heavily underestimated interception, leading to high values of soil evaporation and groundwater transpiration.

Flows (mm)	Obs.	BIOME	LEACHM	TETIS-CN
Precipitation	426.2	426.2	-	426.2
Interception	129.2	129.5	-	81.4
Net precipitation	297.1	296.7	297.1	344.8
Soil evaporation	-	34.4	64.4	118.7
Soil transpiration	-	49.9	68.9	49.6
Groundwater transpiration	-	22.2	21.0	44.2
Total transpiration	101.6	72.1	89.9	93.7
Runoff	4.6	4.0	3.0	0.0
Net percolation	-	188.5	140.8	137.5

Table *4* Mean annual water balances (2012-2015).

On the other hand, the performance of the models in reproducing the carbon and nitrogen field observations after the calibration process was acceptable (Fig. 7). Accumulated mineralization and nitrification were well reproduced taking into account the standard deviation of the measurements (Fig. 8 and Fig. 9). The three models presented almost all simulated values within the limits of the standard deviation; however, BIOME showed mineralization values below the average and both, BIOME and LEACHM had a low temporal variability which led to a low value of dispersion (Fig. 12) in reproducing mineralization and nitrification. TETIS-CN was able to reproduce the observed values and the trend, but it overestimated mineralization and nitrification from October to November, which correspond with the outlier values in Fig. 12.

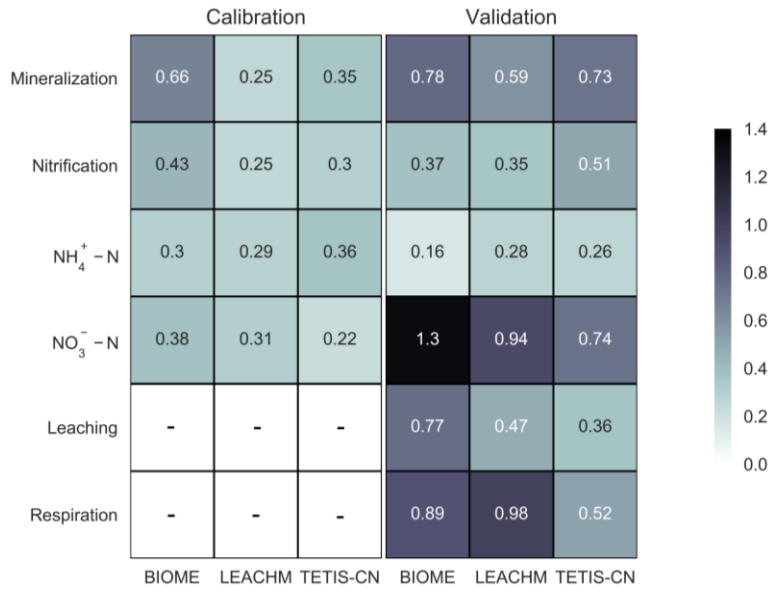

Figure 7 Heatmap representation of accumulated net mineralization, accumulated net nitrification, NH_4^+-N soil content, NO_3^--N soil content, accumulated mineral nitrogen leaching and heterotrophic soil respiration RMSE indices.

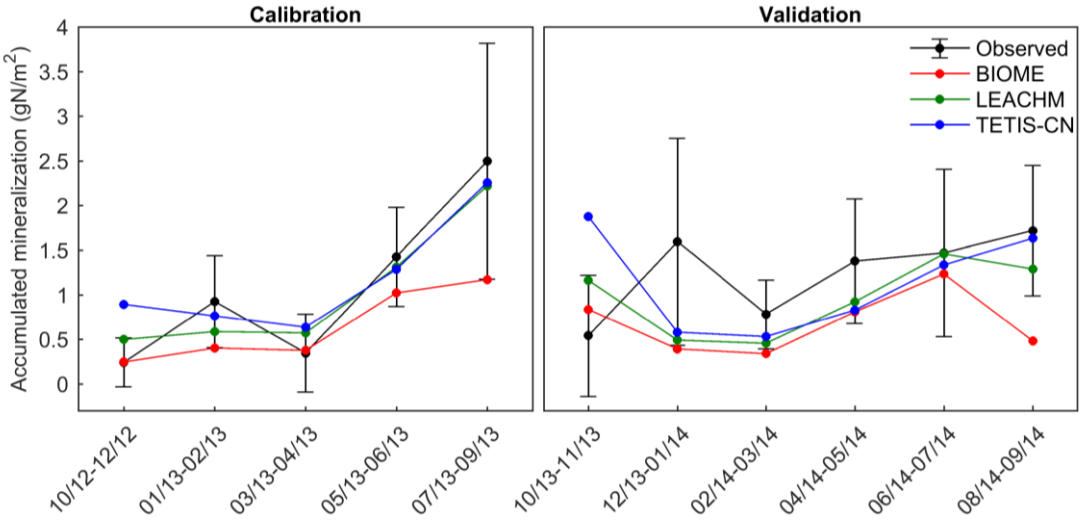

Figure 8 Spatially averaged observed values and simulated values of accumulated mineralization.

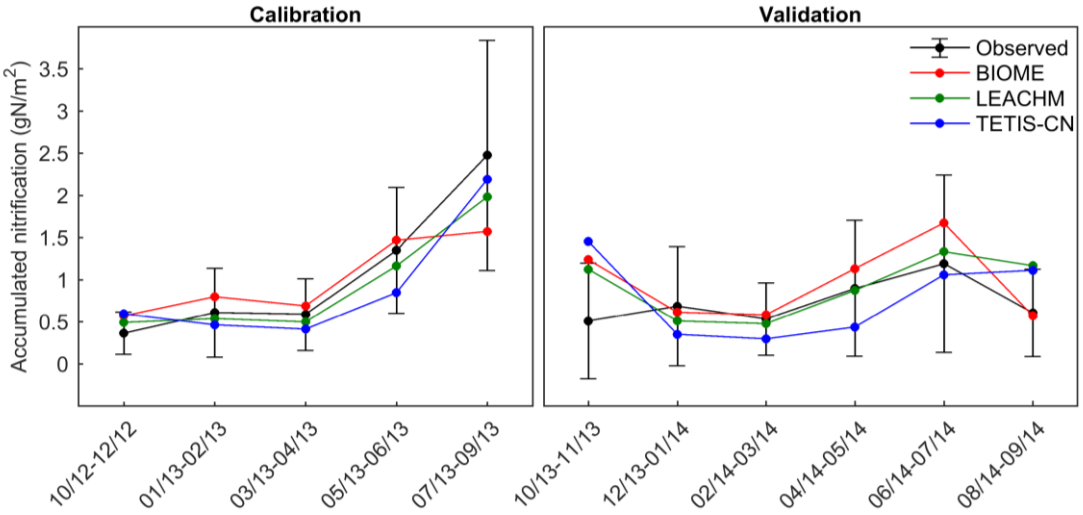

Figure 9 Spatially averaged observed values and simulated values of accumulated nitrification.

Concerning the NH_4^+-N soil content, the three models showed an acceptable performance taking into account the standard deviation of the measurements (Fig. 10). BIOME and LEACHM presented better results, but both were very stable, showing lower dispersions than the observed one (Fig. 12). TETIS-CN overestimated the NH_4^+-N soil content during the warmest months, from June to September, but it was able to maintain a median and dispersion similar to the observed one (Fig.12).

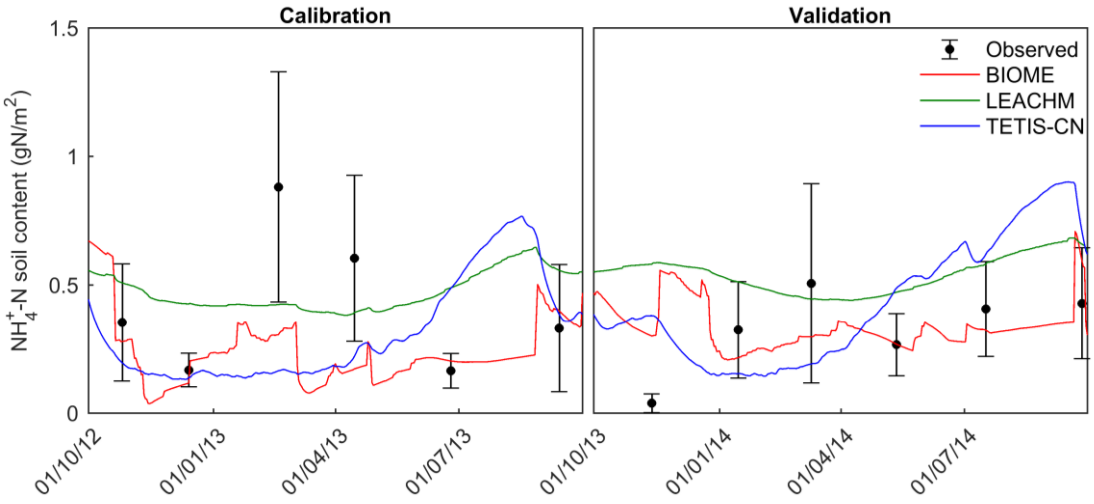

Figure 10 Spatially averaged observed values and simulated values of NH_4^+-N soil content

In the case of the NO_3^--N soil content, the performance of the models was poor, especially during the validation period (Fig. 7 and Fig. 11). The maximum simulated values and the dispersion were well above the observed ones (Fig. 12). Specifically, this problem was found during the periods with scarce precipitation events (Fig. 11), from June to November of 2013 and from April to September of 2014 (the 2013-2014 hydrological year was very dry, with a precipitation of 271.1 mm, compared to the 581.2 mm of the 2012-2013 hydrological year). The best results were obtained by TETIS-CN, but no noteworthy differences were found between the three models.

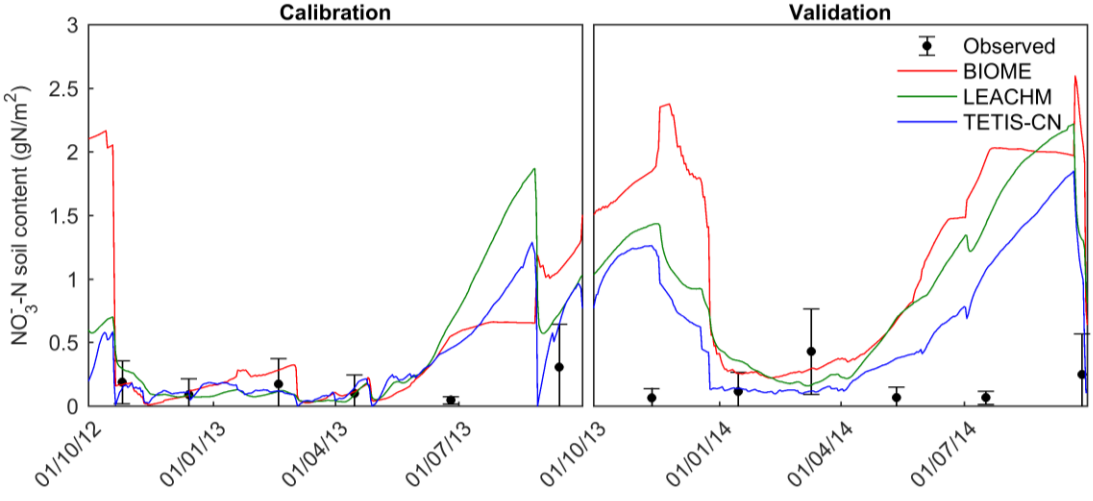

Figure 11 Spatially averaged observed values and simulated values of NO_3^--N soil content

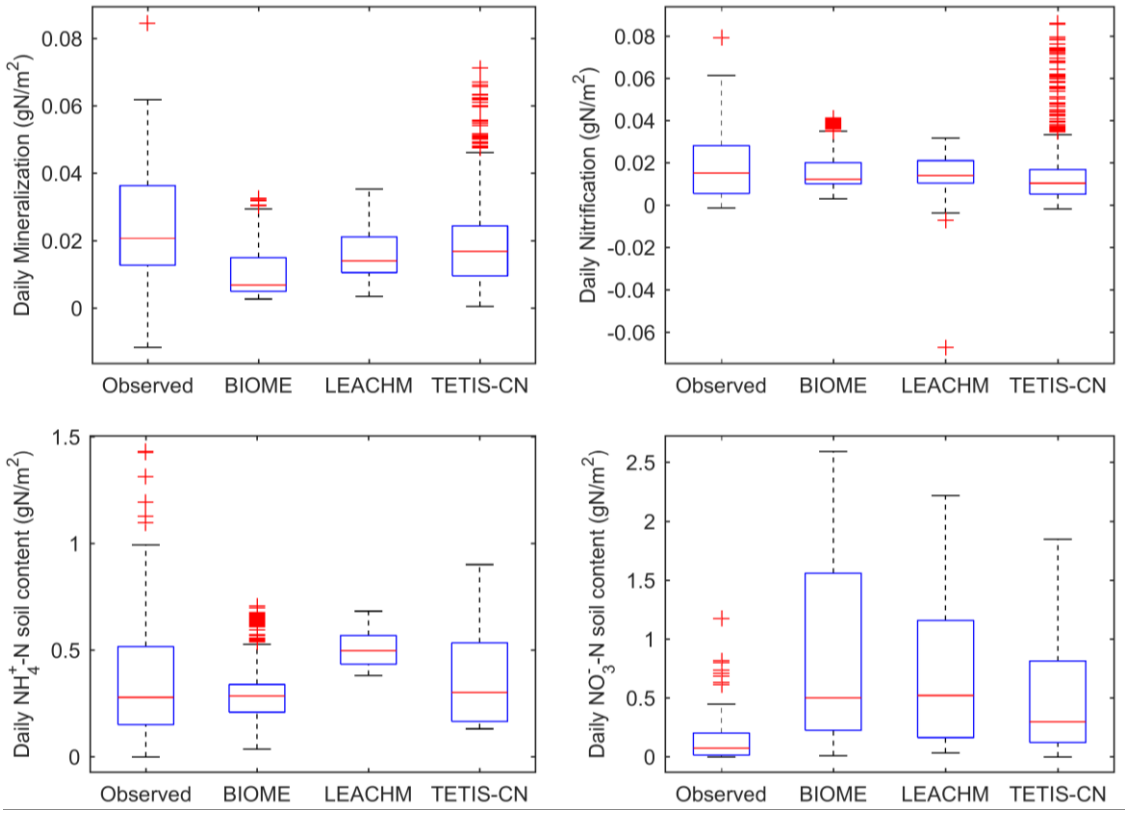

Figure 12 Mineralization, nitrification, NH_4^+-N soil content and NO_3^--N soil content box plots of the spatial and temporal observed values and simulated values.

Regarding soil respiration, neither BIOME nor LEACHM were able to reproduce the heterotrophic respiration (Fig. 7). Both models obtained respiration values below the observed ones and they did not reproduce the trend (Fig. 13).

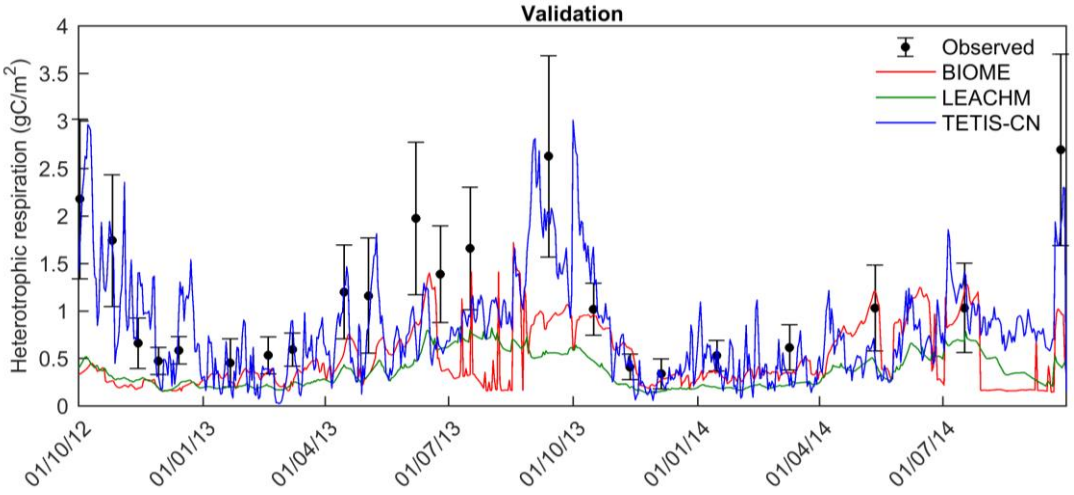

Figure 13 Spatially averaged observed values and simulated values of heterotrophic respiration

Accumulated leaching (Fig. 14) was heavily overestimated during the periods with high precipitation events. Particularly this problem was shown in the case of BIOME, whilst LEACHM and TETIS-CN showed better results.

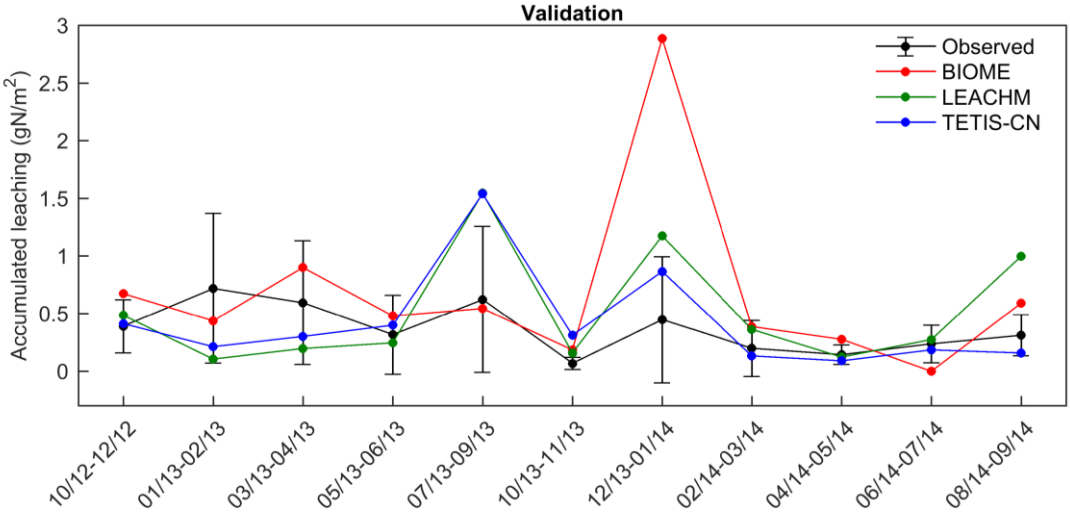

Figure 14 Spatially averaged observed values and simulated values of accumulated mineral nitrogen leaching

Finally, some differences were found in the mean annual balances (Table 5). These were found in the organic carbon plant residue, heterotrophic soil respiration (CO_2 release), plant uptake and leaching. BIOME and LEACHM obtained lower values of organic carbon plant residue input and heterotrophic respiration. However, TETIS-CN values of heterotrophic respiration were closer to the observed ones (Fig. 7 and Fig. 13), according to the partition between autotrophic and heterotrophic respiration of Hanson et al. (2000). Moreover, BIOME obtained higher values of leaching and lower values of plant uptake, but the leaching values of LEACHM and TETIS-CN were closer to the observed ones (Fig. 7 and Fig. 14).

Fluxes	BIOME	LEACHM	TETIS-CN
Organic carbon plant residue (gC m^{-2})	152.75	112.95	262.53
Heterotrophic soil respiration (gC m^{-2})	182.86	135.48	292.21
Organic nitrogen plant residue (gN m^{-2})	3.28	5.23	9.07
Net mineralization (gN m^{-2})	3.80	5.77	6.93
Volatilization (gN m^{-2})	0.00	0.11	0.00
Net nitrification (gN m^{-2})	5.66	5.34	5.28
Denitrification (gN m^{-2})	0.33	0.11	0.26
NH_4^+-N plant uptake (gN m^{-2})	0.07	0.07	1.23
NO_3^--N plant uptake (gN m^{-2})	0.24	1.91	2.23

NH_4^+-N leaching (gN m^{-2})	1.58	0.07	0.09
NO_3^--N leaching (gN m^{-2})	4.36	3.44	3.08

Table *5* Mean annual carbon and nitrogen balances in the first 15 cm of soil (2012-2014)

4 Discussion

Regarding the general water dynamics, BIOME was the only model which heavily worsened its performance during the validation period. This problem may be explained by its high parameter requirements, problem known as model over-parameterization. A simple model may not make the best use of data; nonetheless, a model with a high number of parameters may fit the data in the calibration period accurately and then, have a bad performance in the validation period (Walker et al., 2003). Conversely, simpler models as LEACHM and TETIS-CN were unable to reproduce the soil water content and transpiration during the driest and warmest months (June to September), disagreements that may be explained by their simple representation of transpiration (Puertes et al., 2019). LEACHM uses weekly reference evapotranspiration values, and TETIS-CN only divides the soil into two layers, which may be oversimplified. Moreover, neither LEACHM nor TETIS-CN include the Vapour Pressure Deficit (VPD) influence in the calculation of transpiration and in this case, transpiration was mainly explained by variations in VPD (del Campo et al., 2019a).

The main difference regarding the water balance was found in the evapotranspiration partitioning. BIOME and LEACHM reached soil evaporation values close to the range obtained by del Campo et al. (2019a) in this same plot, which was 43-51 mm $year^{-1}$, and similar groundwater transpiration values, but the 20 mm difference in soil transpiration was substantial. Nevertheless, BIOME underestimated total transpiration in 30 mm approximately, which may be explained by the joint hydrology and biogeochemistry calibration process. In the case of BIOME, the hydrology performance of the model may have been decreased by a better biogeochemistry performance because when more than one objective is included in a calibration process, an improvement in the representation of one causes deterioration in the other one (Vrugt et al., 2003).

584 Conversely, TETIS-CN underestimated interception in almost 50 mm year^{-1}, which led to
585 a very high value of soil evaporation. Its interception modelling is simple and depends
586 on LAI values, which corresponded to corrected satellite LAI values, not being completely
587 representative of the real plot's LAI. As MODIS cell size is 500 m it includes not only the
588 study plot. In contrast, even though LEACHM does not consider vegetation growth, as it
589 does not simulates the process of interception, it did not show this problem. Additionally,
590 TETIS-CN reached a higher value of groundwater transpiration, but the values obtained
591 by the three models were in the range of previous studies developed under semiarid
592 climates (Puertes et al., 2019).
593 In terms of biogeochemistry, the models showed different mean annual values of organic
594 carbon and nitrogen plant residue inputs. BIOME and LEACHM presented a similar value
595 of organic carbon plant residue input, and as in mature natural forests inputs and outputs
596 are generally balanced (Porporato et al., 2003), this value was similar to their
597 heterotrophic soil respiration (CO_2 release). Conversely, TETIS-CN reached higher
598 values, but its heterotrophic soil respiration was closer to the estimated punctual
599 observations, suggesting that BIOME and LEACHM underestimated the organic carbon
600 content of the plant residues, and due to the equilibrium, the heterotrophic soil
601 respiration. This poor performance may be explained by a conceptualization error, a poor
602 description of soil organic matter decomposition or more probably, because no carbon
603 measurement was included in the calibration process. The available observations may
604 not be enough to measure all the characteristics of the system, and thus, their
605 performance may increase if some additional carbon measurements are included as
606 constraints (Uhlenbrook and Sieber, 2005). In fact, in the case of LEACHM, it has been
607 widely used in studies for simulating nitrogen transformation, but these studies rarely
608 consider measured and simulated carbon changes (Mittal et al., 2007) and Asada et al.
609 (2013) modified the model in order to obtain a better description of soil organic matter
610 decomposition. Additionally, as a balanced system, the differences in the organic
611 nitrogen plant residue input between models are associated to the different

612 mineralization values, but these differences were only noteworthy for TETIS-CN from
613 October to November, when mineralization was overestimated. Its correction functions
614 of soil water content and temperature vary in a wider range and consequently, BIOME
615 and LEACHM are more stable. However, in both years 2012 and 2013, during the month
616 of October, the temperature was still elevated, and as it rained, mineralization was
617 overestimated in TETIS-CN.
618 Regarding plant uptake and leaching, the results were very different. Since BIOME
619 includes plant growth, the model simulated root growth towards deep layers (8 m depth),
620 were water was available, reducing the percentage of roots in the first 15 cm of soil and
621 consequently, the nitrogen plant uptake from these soil layers. Conversely, roots depth
622 in LEACHM and TETIS-CN were smaller, being the percentage in these first 15 cm of
623 soil higher. LEACHM potential uptake in the first 15 cm was 26.77 kgN ha^{-1} $year^{-1}$, while
624 TETIS-CN was 39.69 kgN ha^{-1} $year^{-1}$, resulting in a higher plant uptake and smaller
625 leaching than the other two models. Therefore, all these results suggest that NO_3^--N plant
626 uptake could be underestimated, and consequently the models showed a leaching
627 overestimation (Verburg and Johnson, 2001).
628 In line with this, NO_3^--N soil content was heavily overestimated during the warm months
629 with scarce precipitation, reinforcing the idea that $NO3^-$-N plant uptake was not properly
630 represented, because nitrification measurements were well represented, which is the
631 only NO_3^--N input considered, denitrification is not a noteworthy flux and leaching was
632 overestimated only during these months. Firstly, this can be explained because in this
633 plot, *Q. ilex* coexists with other species, which were not considered in this case study.
634 These nitrogen field measurements are representative of the first 15 cm of soil, and
635 although *Q. faginea* and *P. halepensis* have deeper root systems (Baquedano and
636 Castillo, 2007), it should be highlighted that *J. oxycedrus* and *J. phoenicea* have shallow
637 root systems (Castillo et al., 2002; Gazol et al., 2017), especially the former, which
638 develops most of its roots in the first 15 cm of soil (Castillo et al., 2002). Therefore, the
639 NO_3^--N plant uptake by other species, not considered here, may be significant. Secondly,

640 the consideration of a fixed daily potential uptake may have led to an oversimplified
641 representation of the nitrogen plant uptake in the case of LEACHM and TETIS-CN. Due
642 to the seasonal variations of VPD in Mediterranean areas, during the warm periods,
643 which coincides with the growing season, transpiration is higher, especially in spring
644 when soil water is not too limiting (Limousin et al., 2009), and consequently *Q.ilex* NO_3^--
645 N plant uptake also changes seasonally (Bonilla and Rodà, 1992). Thus, considering a
646 fixed daily potential uptake may become an error in the conceptualization that could
647 probably be solved coupling the models to a vegetation growth model. However, in spite
648 of considering vegetation growth, BIOME presented the same problem making the first
649 option more probable.

650 ## 5 Conclusions

651 In this study, three carbon and nitrogen models, with different conceptualization,
652 complexity and purpose, were calibrated in an experimental *Q. ilex* forest plot, with two
653 objectives. Firstly, contributing to a better understanding and modelling of the
654 hydrological and biogeochemical cycles (carbon and nitrogen) and their interaction within
655 the soil-plant continuum in semiarid conditions, and secondly, testing the capability of a
656 new parsimonious carbon and nitrogen sub-model to satisfactorily reproduce them. In
657 this sense, the three models were able to reproduce the hydrological behaviour of a *Q.*
658 *ilex* forest. However, BIOME presented over-parameterization problems, decreasing its
659 performance during the validation period and TETIS-CN showed a higher dependence
660 of *Q. ilex* on groundwater resources. Due to its simple representation of interception, it
661 was underestimated and soil evaporation was overestimated. Therefore, it is clear this
662 problem could be solved if its vegetation dynamic sub-model is used (i.e., considering
663 the vegetation growth).
664 In terms of biogeochemistry, BIOME and LEACHM showed an underestimation of the
665 organic carbon plant residue input, and consequently also of the heterotrophic soil
666 respiration. This was probably caused because no carbon measurement was included

667 in the calibration process and the available measurements were not enough to measure
668 all the characteristics of the system. Therefore, if no carbon measurement is available
669 the nitrogen performance of these models may be good, but the carbon cycle may not
670 be properly reproduced. In the case of TETIS-CN, the default parameters were able to
671 satisfactorily reproduce the heterotrophic respiration measurements in this case study,
672 but in other applications, it may present this same problem. Regarding to the nitrogen
673 performance of the models, NO_3^--N soil content and mineral nitrogen leaching were
674 overestimated, suggesting that NO_3^--N plant uptake may be underestimated. This
675 problem may be firstly explained because *Q. ilex* coexists with other species with a
676 different behaviour whose plant uptake may be significant. Secondly, in the case of
677 LEACHM and TETIS-CN, a fixed daily potential uptake may not be appropriate to
678 reproduce plant nitrogen uptake, which presents a clear seasonality. Therefore, it is
679 important to consider all the species, although scarce, and in the case of LEACHM and
680 TETIS-CN, to couple them to a vegetation growth model.
681 Finally, it is worth noting that none of the models stood out from the rest in reproducing
682 the hydrology and the biogeochemistry of this experimental plot. Hence, the similarity
683 between the results demonstrates that TETIS-CN, with a lower number of parameters,
684 is an acceptable tool to be applied to reproduce the carbon and nitrogen dynamics in
685 Mediterranean drylands.

686 **Acknowledgements**

687 This work was supported by the Spanish Ministry of Science and Innovation through the
688 research projects: TETISMED (CGL2014-58127-C3-3-R), SILWAMED (CGL2014-
689 58127-C3-2-R), CEHYRFO-MED (CGL2017-86839-C3-2-R) and TETISCHANGE
690 (RTI2018-093717-B-100), and by the project LIFE17 CCA/ES/000063
691 RESILIENTFORESTS.

692 **References**

693 Abbaspour, K.C., Yang, J., Maximov, I., Siber, R., Bogner, K., Mieleitner, J., Zobrist, J.,

694 Srinivasan, R., 2007. Modelling hydrology and water quality in the pre-alpine/alpine
695 Thur watershed using SWAT. J. Hydrol. 333, 413–430.
696 https://doi.org/10.1016/J.JHYDROL.2006.09.014
697 Aponte, C., Marañón, T., García, L. V., 2010. Microbial C, N and P in soils of
698 Mediterranean oak forests: Influence of season, canopy cover and soil depth.
699 Biogeochemistry 101, 77–92. https://doi.org/10.1007/s10533-010-9418-5
700 Asada, K., Eguchi, S., Tsunekawa, A., Tsuji, M., Itahashi, S., Katou, H., 2015. Predicting
701 nitrogen leaching with the modified LEACHM model: validation in soils receiving
702 long-term application of animal manure composts. Nutr. Cycl. Agroecosystems 102,
703 209–225. https://doi.org/10.1007/s10705-015-9690-9
704 Asada, K., Eguchi, S., Urakawa, R., Itahashi, S., Matsumaru, T., Nagasawa, T., Aoki, K.,
705 Nakamura, K., Katou, H., 2013. Modifying the LEACHM model for process-based
706 prediction of nitrate leaching from cropped Andosols. Plant Soil 373, 609–625.
707 https://doi.org/10.1007/s11104-013-1809-7
708 Austin, A.T., Yahdjian, L., Stark, J.M., Belnap, J., Porporato, A., Norton, U., Ravetta,
709 D.A., Schaeffer, S.M., 2004. Water pulses and biogeochemical cycles in arid and
710 semiarid ecosystems. Oecologia 141, 221–235. https://doi.org/10.1007/s00442-
711 004-1519-1
712 Baquedano, F.J., Castillo, F.J., 2007. Drought tolerance in the Mediterranean species
713 Quercus coccifera, Quercus ilex, Pinus halepensis, and Juniperus phoenicea.
714 Photosynthetica 45, 229–238. https://doi.org/10.1007/s11099-007-0037-x
715 Batlle-Aguilar, J., Brovelli, A., Porporato, A., Barry, D.A., 2011. Modelling soil carbon and
716 nitrogen cycles during land use change. A review. Agron. Sustain. Dev. 31, 251–
717 274. https://doi.org/10.1051/agro/2010007
718 Bautista, I., Pabón, C., Lull, C., González-Sanchís, M., Lidón, A., Del Campo, A.D., 2015.
719 Efectos de la gestión forestal en los flujos de nutrientes asociados al ciclo
720 hidrológico en un bosque mediterráneo de Quercus Ilex. Cuad. la Soc. Española
721 Ciencias For. 41, 343–354.

722 Blanco, J.A., Zavala, M.A., Imbert, J.B., Castillo, F.J., 2005. Sustainability of forest
723 management practices: Evaluation through a simulation model of nutrient cycling.
724 For. Ecol. Manage. 213, 209–228. https://doi.org/10.1016/j.foreco.2005.03.042
725 Bonilla, D., Rodà, F., 1992. Soil nitrogen dynamics in a holm oak forest. Vegetatio 99–
726 100, 247–257. https://doi.org/10.1007/BF00118231
727 Botter, G., Daly, E., Porporato, A., Rodriguez-Iturbe, I., Rinaldo, A., 2008. Probabilistic
728 dynamics of soil nitrate: Coupling of ecohydrological and biogeochemical
729 processes. Water Resour. Res. 44, 15. https://doi.org/10.1029/2007WR006108
730 Burgess, S.S.O., Adams, M.A., Turner, N.C., Beverly, C.R., Ong, C.K., Khan, A.A.,
731 Bleby, T.M., 2001. An improved heat pulse method to measure low and reverse
732 rates of sap flow in woody plants. Tree Physiol. 21, 589–98.
733 Calama, R., Conde, M., De-Dios-García, J., Madrigal, G., Vázquez-Piqué, J., Gordo,
734 F.J., Pardos, M., 2019. Linking climate, annual growth and competition in a
735 Mediterranean forest: Pinus pinea in the Spanish Northern Plateau. Agric. For.
736 Meteorol. 264, 309–321. https://doi.org/10.1016/j.agrformet.2018.10.017
737 Campbell, G.S., 1974. A simple method for determining unsaturated conductivity from
738 moisture retention data. Soil Sci. 117, 311–314. https://doi.org/10.1097/00010694-
739 197406000-00001
740 Castillo, J.M., Rubio Casal, A.E., Luque, C.J., Luque, T., Figueroa, M.E., 2002.
741 Comparative field summer stress of three tree species co-occurring in
742 Mediterranean coastal dunes. Photosynthetica 40, 49–56.
743 https://doi.org/10.1023/A:1020133921204
744 Chen, Y., Xiao, W., 2019. Estimation of Forest NPP and Carbon Sequestration in the
745 Three Gorges Reservoir Area, Using the Biome-BGC Model. Forests 10, 17.
746 https://doi.org/10.3390/f10020149
747 Chiesi, M., Maselli, F., Moriondo, M., Fibbi, L., Bindi, M., Running, S.W., 2007.
748 Application of BIOME-BGC to simulate Mediterranean forest processes. Ecol.
749 Modell. 206, 179–190. https://doi.org/10.1016/j.ecolmodel.2007.03.032

Contreras, W.A., Lidón, A.L., Ginestar, D., Bru, R., 2009. Compartmental model for nitrogen dynamics in citrus orchards. Math. Comput. Model. 50, 794–805. https://doi.org/10.1016/j.mcm.2009.05.008

D'Odorico, P., Laio, F., Porporato, A., Rodriguez-Iturbe, I., 2003. Hydrologic controls on soil carbon and nitrogen cycles. II. A case study. Adv. Water Resour. 26, 59–70. https://doi.org/10.1016/S0309-1708(02)00095-7

D'Odorico, P., Porporato, A., Laio, F., Ridolfi, L., Rodriguez-Iturbe, I., 2004. Probabilistic modeling of nitrogen and carbon dynamics in water-limited ecosystems, in: Ecological Modelling. Elsevier, pp. 205–219. https://doi.org/10.1016/j.ecolmodel.2004.06.005

del Campo, A.D., González-Sanchis, M., García-Prats, A., Ceacero, C.J., Lull, C., 2019a. The impact of adaptive forest management on water fluxes and growth dynamics in a water-limited low-biomass oak coppice. Agric. For. Meteorol. 264, 266–282. https://doi.org/10.1016/j.agrformet.2018.10.016

del Campo, A.D., González-Sanchis, M., Lidón, A., Ceacero, C.J., García-Prats, A., 2018. Rainfall partitioning after thinning in two low-biomass semiarid forests: Impact of meteorological variables and forest structure on the effectiveness of water-oriented treatments. J. Hydrol. 565, 74–86. https://doi.org/10.1016/J.JHYDROL.2018.08.013

del Campo, A.D., González-Sanchis, M., Molina, A.J., García-Prats, A., Ceacero, C.J., Bautista, I., 2019b. Effectiveness of water-oriented thinning in two semiarid forests: The redistribution of increased net rainfall into soil water, drainage and runoff. For. Ecol. Manage. 438, 163–175. https://doi.org/10.1016/J.FORECO.2019.02.020

DiStefano, J.F., Gholz, H.L., 1986. A proposed use of ion exchange resins to measure nitrogen mineralization and nitrification in intact soil cores. Commun. Soil Sci. Plant Anal. 17, 989–998. https://doi.org/10.1080/00103628609367767

Doherty, J., 2007. Users Manual for PEST Version 11. Watermark Numer. Comput., Brisbane, Queensl., Australia.

778 Dong, Z., Driscoll, C.T., Johnson, S.L., Campbell, J.L., Pourmokhtarian, A., Stoner,
779 A.M.K., Hayhoe, K., 2019. Projections of water, carbon, and nitrogen dynamics
780 under future climate change in an old-growth Douglas-fir forest in the western
781 Cascade Range using a biogeochemical model. Sci. Total Environ. 656, 608–624.
782 https://doi.org/10.1016/j.scitotenv.2018.11.377
783 Farquhar, G.D., von Caemmerer, S., Berry, J.A., 1980. A biochemical model of
784 photosynthetic CO2 assimilation in leaves of C3 species. Planta 149, 78–90.
785 https://doi.org/10.1007/BF00386231
786 Fierer, N., Schimel, J.P., Holden, P.A., 2003. Variations in microbial community
787 composition through two soil depth profiles. Soil Biol. Biochem. 35, 167–176.
788 https://doi.org/10.1016/S0038-0717(02)00251-1
789 Fontes, L., Bontemps, J.-D., Bugmann, H., Van Oijen, M., Gracia, C., Kramer, K.,
790 Lindner, M., Rötzer, T., Skovsgaard, J.P., 2010. Models for supporting forest
791 management in a changing environment. For. Syst. 19, 8–29.
792 https://doi.org/10.5424/fs/201019s-9315
793 Francés, F., Vélez, J.I., Vélez, J.J., 2007. Split-parameter structure for the automatic
794 calibration of distributed hydrological models. J. Hydrol. 332, 226–240.
795 https://doi.org/10.1016/J.JHYDROL.2006.06.032
796 Gazol, A., Sangüesa-Barreda, G., Granda, E., Camarero, J.J., 2017. Tracking the impact
797 of drought on functionally different woody plants in a Mediterranean scrubland
798 ecosystem. Plant Ecol. 218, 1009–1020. https://doi.org/10.1007/s11258-017-0749-
799 3
800 Gleeson, D., Mathes, F., Farrell, M., Leopold, M., 2016. Environmental drivers of soil
801 microbial community structure and function at the Avon River Critical Zone
802 Observatory. Sci. Total Environ. 571, 1407–1418.
803 https://doi.org/10.1016/J.SCITOTENV.2016.05.185
804 Hanson, P.J., Edwards, N.T., Garten, C.T., Andrews, J.A., 2000. Separating root and
805 soil microbial contributions to soil respiration: A review of methods and

observations. Biogeochemistry 48, 115–146. https://doi.org/10.1023/A:1006244819642

Härkönen, S., Neumann, M., Mues, V., Berninger, F., Bronisz, K., Cardellini, G., Chirici, G., Hasenauer, H., Koehl, M., Lang, M., Merganicova, K., Mohren, F., Moiseyev, A., Moreno, A., Mura, M., Muys, B., Olschofsky, K., Del Perugia, B., Rørstad, P.K., Solberg, B., Thivolle-Cazat, A., Trotsiuk, V., Mäkelä, A., 2019. A climate-sensitive forest model for assessing impacts of forest management in Europe. Environ. Model. Softw. 115, 128–143. https://doi.org/10.1016/j.envsoft.2019.02.009

Hidy, D., Barcza, Z., Marjanović, H., Ostrogović Sever, M.Z., Dobor, L., Gelybó, G., Fodor, N., Pintér, K., Churkina, G., Running, S., Thornton, P., Bellocchi, G., Haszpra, L., Horváth, F., Suyker, A., Nagy, Z., 2016. Terrestrial ecosystem process model Biome-BGCMuSo v4.0: summary of improvements and new modeling possibilities. Geosci. Model Dev. 9, 4405–4437. https://doi.org/10.5194/gmd-9-4405-2016

Hutson, J.L., 2003. LEACHM - Leaching Estimation and Chemistry Model. Department of Crop and Soil Sciences, Cornell University, Ithaca, New York, Ithaca, New York.

Jenkinson, D.S., Andrew, S.P.S., Lynch, J.M., Goss, M.J., Tinker, P.B., 1990. The turnover of organic carbon and nitrogen in soil. Philos. Trans. R. Soc. London. Ser. B Biol. Sci. 329, 361–368. https://doi.org/10.1098/rstb.1990.0177

Jin, W., He, H.S., Thompson, F.R., 2016. Are more complex physiological models of forest ecosystems better choices for plot and regional predictions? Environ. Model. Softw. 75, 1–14. https://doi.org/10.1016/j.envsoft.2015.10.004

Jung, Y.W., Oh, D.S., Kim, M., Park, J.W., 2010. Calibration of LEACHN model using LH-OAT sensitivity analysis. Nutr. Cycl. Agroecosystems 87, 261–275. https://doi.org/10.1007/s10705-009-9337-9

Kätterer, T., Andrén, O., 2001. The ICBM family of analytically solved models of soil carbon, nitrogen and microbial biomass dynamics - descriptions and application examples. Ecol. Modell. 136, 191–207. https://doi.org/10.1016/S0304-

834 3800(00)00420-8
835 Lado-Monserrat, L., Lull, C., Bautista, I., Lidón, A., Herrera, R., 2014. Soil moisture
836 increment as a controlling variable of the “Birch effect”. Interactions with the pre-
837 wetting soil moisture and litter addition. Plant Soil 379, 21–34.
838 https://doi.org/10.1007/s11104-014-2037-5
839 Landsberg, J., 2003. Modelling forest ecosystems: state of the art, challenges, and future
840 directions. Can. J. For. Res. 33, 385–397. https://doi.org/10.1139/x02-129
841 Lardy, R., Bellocchi, G., Soussana, J.F., 2011. A new method to determine soil organic
842 carbon equilibrium. Environ. Model. Softw. 26, 1759–1763.
843 https://doi.org/10.1016/j.envsoft.2011.05.016
844 Lidón, A., Ramos, C., Ginestar, D., Contreras, W., 2013. Assessment of LEACHN and a
845 simple compartmental model to simulate nitrogen dynamics in citrus orchards.
846 Agric. Water Manag. 121, 42–53. https://doi.org/10.1016/j.agwat.2013.01.008
847 Limousin, J.M., Rambal, S., Ourcival, J.M., Rocheteau, A., Joffre, R., Rodriguez-Cortina,
848 R., 2009. Long-term transpiration change with rainfall decline in a Mediterranean
849 Quercus ilex forest. Glob. Chang. Biol. 15, 2163–2175.
850 https://doi.org/10.1111/j.1365-2486.2009.01852.x
851 Lozano-García, B., Parras-Alcántara, L., Brevik, E.C., 2016. Impact of topographic
852 aspect and vegetation (native and reforested areas) on soil organic carbon and
853 nitrogen budgets in Mediterranean natural areas. Sci. Total Environ. 544, 963–970.
854 https://doi.org/10.1016/j.scitotenv.2015.12.022
855 Lü, X.-T., Liu, Z.-Y., Hu, Y.-Y., Zhang, H.-Y., 2018. Testing nitrogen and water co-
856 limitation of primary productivity in a temperate steppe. Plant Soil 432, 119–127.
857 https://doi.org/10.1007/s11104-018-3791-6
858 Lucas-Borja, M.E., Hedo de Santiago, J., Yang, Y., Shen, Y., Candel-Pérez, D., 2019.
859 Nutrient, metal contents and microbiological properties of litter and soil along a tree
860 age gradient in Mediterranean forest ecosystems. Sci. Total Environ. 650, 749–758.
861 https://doi.org/10.1016/j.scitotenv.2018.09.079

862 Manzoni, S., Porporato, A., 2007. A theoretical analysis of nonlinearities and feedbacks
863 in soil carbon and nitrogen cycles. Soil Biol. Biochem. 39, 1542–1556.
864 https://doi.org/10.1016/j.soilbio.2007.01.006
865 Manzoni, S., Porporato, A., D'Odorico, P., Laio, F., Rodriguez-Iturbe, I., 2004. Soil
866 nutrient cycles as a nonlinear dynamical system. Nonlinear Process. Geophys. 11,
867 589–598. https://doi.org/10.5194/npg-11-589-2004
868 Medici, C., Butturini, A., Bernal, S., Vázquez, E., Sabater, F., Vélez, J.I., Francés, F.,
869 2008. Modelling the non-linear hydrological behaviour of a small Mediterranean
870 forested catchment. Hydrol. Process. 22, 3814–3828.
871 https://doi.org/10.1002/hyp.6991
872 Medici, C., Wade, A.J., Francés, F., 2012. Does increased hydrochemical model
873 complexity decrease robustness? J. Hydrol. 440–441, 1–13.
874 https://doi.org/10.1016/j.jhydrol.2012.02.047
875 Mertens, J., Madsen, H., Kristensen, M., Jacques, D., Feyen, J., 2005. Sensitivity of soil
876 parameters in unsaturated zone modelling and the relation between effective,
877 laboratory and in situ estimates. Hydrol. Process. 19, 1611–1633.
878 https://doi.org/10.1002/hyp.5591
879 Mittal, S.B., Anlauf, R., Laik, R., Gupta, A.P., Kapoor, A.K., Dahiya, S.S., 2007. Modeling
880 nitrate leaching and organic-C build-up under semi-arid cropping conditions of N
881 India. J. Plant Nutr. Soil Sci. 170, 506–513. https://doi.org/10.1002/jpln.200521725
882 Moriasi, D.N., Arnold, J.G., Van Liew, M.W., Bingner, R.L., Harmel, R.D., Veith, T.L.,
883 2007. Model Evaluation Guidelines for Systematic Quantification of Accuracy in
884 Watershed Simulations. Trans. ASABE 50, 885–900.
885 https://doi.org/10.13031/2013.23153
886 Nasri, N., Chebil, M., Guellouz, L., Bouhlila, R., Maslouhi, A., Ibnoussina, M., 2015.
887 Modelling nonpoint source pollution by nitrate of soil in the Mateur plain, northeast
888 of Tunisia. Arab. J. Geosci. 8, 1057–1075. https://doi.org/10.1007/s12517-013-
889 1215-8

890 Newman, G.S., Arthur, M.A., Muller, R.N., 2006. Above- and belowground net primary
891 production in a temperate mixed deciduous forest. Ecosystems 9, 317–329.
892 https://doi.org/10.1007/s10021-006-0015-3
893 Nimah, M.N., Hanks, R.J., 1973. Model for Estimating Soil Water, Plant, and
894 Atmospheric Interrelations: I. Description and Sensitivity. Soil Sci. Soc. Am. J. 37,
895 522–527. https://doi.org/10.2136/sssaj1973.03615995003700040018x
896 Pasquato, M., Medici, C., Friend, A.D., Francés, F., 2015. Comparing two approaches
897 for parsimonious vegetation modelling in semiarid regions using satellite data.
898 Ecohydrology 8, 1024–1036. https://doi.org/10.1002/eco.1559
899 Pastor, J., Post, W.M., 1986. Influence of climate, soil moisture, and succession on forest
900 carbon and nitrogen cycles. Biogeochemistry 2, 3–27.
901 https://doi.org/10.1007/BF02186962
902 Porporato, A., D'Odorico, P., Laio, F., Rodriguez-Iturbe, I., 2003. Hydrologic controls on
903 soil carbon and nitrogen cycles. I. Modeling scheme. Adv. Water Resour. 26, 45–
904 58. https://doi.org/10.1016/S0309-1708(02)00094-5
905 Porporato, A., Feng, X., Manzoni, S., Mau, Y., Parolari, A.J., Vico, G., 2015.
906 Ecohydrological modeling in agroecosystems: Examples and challenges. Water
907 Resour. Res. 51, 5081–5099. https://doi.org/10.1002/2015WR017289
908 Puertes, C., Lidón, A., Echeverría, C., Bautista, I., González-Sanchis, M., del Campo,
909 A.D., Francés, F., 2019. Explaining the hydrological behaviour of facultative
910 phreatophytes using a multi-variable and multi-objective modelling approach. J.
911 Hydrol. 575, 395–407. https://doi.org/10.1016/j.jhydrol.2019.05.041
912 Ramos, C., Carbonell, E.A., 1991. Nitrate leaching and soil moisture prediction with the
913 LEACHM model. Fertil. Res. 27, 171–180. https://doi.org/10.1007/BF01051125
914 Rodrigo, A., Recous, S., Neel, C., Mary, B., 1997. Modelling temperature and moisture
915 effects on C-N transformations in soils: Comparison of nine models. Ecol. Modell.
916 102, 325–339. https://doi.org/10.1016/S0304-3800(97)00067-7
917 Ruiz-Pérez, G., González-Sanchis, M., Del Campo, A.D., Francés, F., 2016. Can a

parsimonious model implemented with satellite data be used for modelling the vegetation dynamics and water cycle in water-controlled environments? Ecol. Modell. 324, 45–53. https://doi.org/10.1016/j.ecolmodel.2016.01.002

Running, S.W., Gower, S.T., 1991. FOREST-BGC, A general model of forest ecosystem processes for regional applications. II. Dynamic carbon allocation and nitrogen budgets. Tree Physiol. 9, 147–160. https://doi.org/10.1093/treephys/9.1-2.147

Sardans, J., Peñuelas, J., 2013. Plant-soil interactions in Mediterranean forest and shrublands: Impacts of climatic change. Plant Soil 365, 1–33. https://doi.org/10.1007/s11104-013-1591-6

Sardans, J., Peñuelas, J., Ogaya, R., 2008. Drought-induced changes in C and N stoichiometry in a Quercus ilex Mediterranean forest. For. Sci. 54, 513–522. https://doi.org/10.1093/forestscience/54.5.513

Sardans, J., Rodà, F., 2004. Phosphorus Limitation and Competitive Capacities of Pinus halepensis and Quercus ilex subsp. rotundifolia on Different Soils. Plant Ecol. 174, 305–317. https://doi.org/10.1023/B:VEGE.0000049110.88127.a0

Schmied, B., Abbaspour, K., Schulin, R., 2000. Inverse Estimation of Parameters in a Nitrogen Model Using Field Data. Soil Sci. Soc. Am. J. 64, 533–542. https://doi.org/10.2136/sssaj2000.642533x

Spinoni, J., Vogt, J. V., Naumann, G., Barbosa, P., Dosio, A., 2018. Will drought events become more frequent and severe in Europe? Int. J. Climatol. 38, 1718–1736. https://doi.org/10.1002/joc.5291

Tateno, R., Taniguchi, T., Zhang, J.-G., Shi, W.Y., Zhang, J.G., Du, S., Yamanaka, N., 2017. Net primary production, nitrogen cycling, biomass allocation, and resource use efficiency along a topographical soil water and nitrogen gradient in a semi-arid forest near an arid boundary. Plant Soil 420, 209–222. https://doi.org/10.1007/s11104-017-3390-y

Taylor, J.P., Wilson, B., Mills, M.S., Burns, R.G., 2002. Comparison of microbial numbers and enzymatic activities in surface soils and subsoils using various techniques. Soil

946 Biol. Biochem. 34, 387–401. https://doi.org/10.1016/S0038-0717(01)00199-7
947 Thornton, P.E., Law, B.E., Gholz, H.L., Clark, K.L., Falge, E., Ellsworth, D.S., Goldstein,
948 A.H., Monson, R.K., Hollinger, D., Falk, M., Chen, J., Sparks, J.P., 2002. Modeling
949 and measuring the effects of disturbance history and climate on carbon and water
950 budgets in evergreen needleleaf forests. Agric. For. Meteorol. 113, 185–222.
951 https://doi.org/10.1016/S0168-1923(02)00108-9
952 Uhlenbrook, S., Sieber, A., 2005. On the value of experimental data to reduce the
953 prediction uncertainty of a process-oriented catchment model. Environ. Model.
954 Softw. 20, 19–32. https://doi.org/10.1016/j.envsoft.2003.12.006
955 Uscola, M., Villar-Salvador, P., Oliet, J., Warren, C.R., 2017. Root uptake of inorganic
956 and organic N chemical forms in two coexisting Mediterranean forest trees. Plant
957 Soil 415, 387–392. https://doi.org/10.1007/s11104-017-3172-6
958 Verburg, P.S.J., Johnson, D.W., 2001. A spreadsheet-based biogeochemical model to
959 simulate nutrient cycling processes in forest ecosystems. Ecol. Modell. 141, 185–
960 200. https://doi.org/10.1016/S0304-3800(01)00273-3
961 Vrugt, J.A., Gupta, H. V., Bastidas, L.A., Bouten, W., Sorooshian, S., 2003. Effective and
962 efficient algorithm for multiobjective optimization of hydrologic models. Water
963 Resour. Res. 39. https://doi.org/10.1029/2002WR001746
964 Walker, W.E., Harremoës, P., Rotmans, J., Van der Sluijs, J.P., Van Asselt, M.B.A.,
965 Janssen, P., Krayer von Krauss, M.P., 2003. Integrated assessment. Integr.
966 Assess. 4, 5–17. https://doi.org/1389-5176/03/0000-000$16.00
967 Wang, C., Wang, S., Fu, B., Li, Z., Wu, X., Tang, Q., 2017. Precipitation gradient
968 determines the tradeoff between soil moisture and soil organic carbon, total
969 nitrogen, and species richness in the Loess Plateau, China. Sci. Total Environ. 575,
970 1538–1545. https://doi.org/10.1016/J.SCITOTENV.2016.10.047
971 Williams, J.R., 1991. Runoff and Water Erosion, in: Modeling Plant and Soil Systems.
972 American Society of Agronomy, Crop Science Society of America, Soil Science
973 Society of America, Madison, WI 53711, USA, pp. 439–455.

https://doi.org/10.2134/agronmonogr31.c18

Wöhling, T., Gayler, S., Priesack, E., Ingwersen, J., Wizemann, H.D., Högy, P., Cuntz, M., Attinger, S., Wulfmeyer, V., Streck, T., 2013. Multiresponse, multiobjective calibration as a diagnostic tool to compare accuracy and structural limitations of five coupled soil-plant models and CLM3.5. Water Resour. Res. 49, 8200–8221. https://doi.org/10.1002/2013WR014536

Woodrow, I.E., Berry, J.A., 1988. Enzymatic regulation of photosynthetic CO2 fixation in C3 Plants. Annu. Rev. Plant Physiol. Plant Mol. Biol. 39, 533–594. https://doi.org/10.1146/annurev.pp.39.060188.002533

Zhang, C., Li, C., Chen, X., Luo, G., Li, L., Li, X., Yan, Y., Shao, H., 2013. A spatial-explicit dynamic vegetation model that couples carbon, water, and nitrogen processes for arid and semiarid ecosystems. J. Arid Land 5, 102–117. https://doi.org/10.1007/s40333-013-0146-2

Appendix A.

Parameter	Units	Value
PLANT FUNCTIONING PARAMETERS		
Transfer growth period as fraction of growing season	Prop.	0.80
Litterfall as fraction of growing season	Prop.	0.80
Base temperature	°C	10
Minimum temperature for growth displayed on current day	°C	0
Optimal1 temperature for growth displayed on current day	°C	11
Optimal2 temperature for growth displayed on current day	°C	28
Maximum temperature for growth displayed on current day	°C	40
Minimum temperature for carbon assimilation displayed on current day	°C	0
Optimal1 temperature for carbon assimilation displayed on current day	°C	12
Optimal2 temperature for carbon assimilation displayed on current day	°C	28
Maximum temperature for carbon assimilation displayed on current day	°C	40
Annual leaf and fine root turnover fraction	yr^{-1}	0.20
Annual live wood turnover fraction	yr^{-1}	0.30
Annual whole-plant mortality fraction	yr^{-1}	0.02
Annual fire mortality fraction	yr^{-1}	0
C:N of leaves	$kgC\ kgN^{-1}$	37.50

C:N of leaf litter, after retranslocation	kgC kgN^{-1}	46.50
C:N of fine roots	kgC kgN^{-1}	43
C:N of fruit	kgC kgN^{-1}	47
C:N of soft stem	kgC kgN^{-1}	0.00
C:N of live wood	kgC kgN^{-1}	73.50
C:N of dead wood	kgC kgN^{-1}	651
Leaf litter labile proportion	[-]	0.20
Leaf litter cellulose proportion	[-]	0.56
Fine root labile proportion	[-]	0.34
Fine root cellulose proportion	[-]	0.44
Fruit litter labile proportion	[-]	0.30
Fruit litter cellulose proportion	[-]	0.29
Soft stem litter labile proportion	[-]	0.00
Soft stem litter cellulose proportion	[-]	0.00
Dead wood cellulose proportion	[-]	0.75
Canopy water interception coefficient	LAI^{-1} d^{-1}	0.25
Canopy light extinction coefficient	[-]	0.36
Potential radiation use efficiency	g MJ^{-1}	2
Radiation parameter1 (Jiang et al.2015)	[-]	0.78
Radiation parameter2 (Jiang et al.2015)	[-]	13.60
All-sided to projected leaf area ratio	[-]	2
Ratio of shaded SLA:sunlit SLA	[-]	2
Fraction of leaf N in Rubisco	[-]	1.13e-2
Fraction of leaf N in PEP Carboxylase	[-]	1e-4
Maximum stomatal conductance (projected area basis)	m s^{-1}	9e-03
Cuticular conductance (projected area basis)	m s^{-1}	7e-04
Boundary layer conductance (projected area basis)	m s^{-1}	5e-4
Relative SWC (prop. to FC) to calc. soil moisture limit 1	Prop.	0.35
Relative SWC (prop. to SAT) to calc. soil moisture limit 2	Prop.	0.68
Relative PSI (prop. to FC) to calc. soil moisture limit 1	Prop.	-9999
Relative PSI (prop. to SAT) to calc. soil moisture limit 2	Prop.	-9999
Vapor pressure deficit: start of conductance reduction	Pa	100
Vapor pressure deficit: complete conductance reduction	Pa	800.78
Maximum height of plant	M	8.50
Stem weight at which maximum height attended	kgC m^{-2}	150
Maximum depth of rooting zone	m	8
Root distribution parameter	[-]	54.48
Root length parameter 1 (estimated max root weight)	kgC m^{-2}	0.40
Root length parameter 2 (slope)	Prop.	0.50
Growth respiration per unit of C grown	Prop.	0.40
Maintenance respiration in kgC/day per kg of tissue N	kgC kgN^{-1} d^{-1}	8.8e-2
Theoretical maximum prop. of non-structural and structural carbohydrates	[-]	0.10
Prop. of non-structural carbohydrates available for maintenance respiration	[-]	0.30
Symbiotic + asymbiotic fixation of N	kgN m^{-2} yr^{-1}	5e-4
SCENESCENCE AND SOIL PARAMETERS		

Maximum senescence mortality coefficient of aboveground plant material	Prop.	0.03
Maximum senescence mortality coefficient of belowground plant material	Prop.	0.03
Maximum senescence mortality coefficient of non-structured plant material	Prop.	0
Effect of extreme high temperature on senescence mortality	Prop.	2
Lower limit extreme high temperature effect on senescence mortality	°C	45
Upper limit extreme high temperature effect on senescence mortality	°C	50
Maximal lifetime of plant tissue	°C	-9999
Turnover rate of wilted standing biomass to litter	Prop.	0.01
Turnover rate of non-woody cut-down biomass to litter	Prop.	0.05
Turnover rate of woody cut-down biomass to litter	Prop.	0.01
Drought tolerance parameter (critical value of DSWS)	Prop.	90
Denitrification rate per g of CO_2 respiration of SOM	Prop.	0.08
Nitrification coefficient 1	Prop.	0.30
Nitrification coefficient 2	Prop.	0.10
Coefficient of N_2O emission of nitrification	Prop.	0.02
Proportion of NH_4 flux of N-deposition	Prop.	0.80
NH_4 mobile proportion	Prop.	0.90
NO_3 mobile proportion	Prop.	1
e-folding depth of decomposition rate's depth scalar	m	10
Fraction of dissolved part of SOIL1 organic matter	Prop.	1e-3
Fraction of dissolved part of SOIL2 organic matter	Prop.	1e-3
Fraction of dissolved part of SOIL3 organic matter	Prop.	1e-3
Fraction of dissolved part of SOIL4 organic matter	Prop.	1e-3
Ratio of bare soil evaporation and pot. evaporation	[-]	10
RATE SCALARS		
Resp. fractions for fluxes between compartments (l1s1)	[-]	0.39
Res. fractions for fluxes between compartments (l2s2)	[-]	0.55
Resp. fractions for fluxes between compartments (l4s3)	[-]	0.29
Resp. fractions for fluxes between compartments (s1s2)	[-]	0.28
Resp. fractions for fluxes between compartments (s2s3)	[-]	0.46
Resp. fractions for fluxes between compartments (s3s4)	[-]	0.55
Rate constant scalar of labile litter pool	[-]	0.70
Rate constant scalar of cellulose litter pool	[-]	0.07
Rate constant scalar of lignin litter pool	[-]	1.40e-2
Rate constant scalar of fast microbial recycling pool	[-]	0.07
Rate constant scalar of medium microbial recycling pool	[-]	1.40e-2
Rate constant scalar of slow microbial recycling pool	[-]	1.40e-3
Rate constant scalar of recalcitrant SOM (humus) pool	[-]	1e-4
Rate constant scalar of physical fragmentation of coarse woody debris	[-]	1e-3
GROWING SEASON PARAMETERS		
Critical amount of snow limiting photosynthesis	kg m^{-2}	5
Limit1 (under:full constrained) of HEATSUM index	°C	20

Limit2 (above:unconstrained) of HEATSUM index	°C	60
Limit1 (under:full constrained) of TMIN index	°C	0
Limit2 (above:unconstrained) of TMIN index	°C	5
Limit1 (above:full constrained) of VPD index	Pa	4000
Limit2 (under:unconstrained) of VPD index	Pa	1000
Limit1 (under:full constrained) of DAYLENGTH index	s	0
Limit2 (above:unconstrained) of DAYLENGTH index	s	0
Moving average (to avoid the effects of extreme events)	day	10
GSI limit1 (greater that limit -> start of vegper)	[-]	0.10
GSI limit2 (less that limit -> end of vegper)	[-]	0.01
CH4 PARAMETERS		
Param1 for CH4 calculations (empirical function of BD)	[-]	212.50
Param2 for CH4 calculations (empirical function of BD)	[-]	1.81
Param1 for CH4 calculations (empirical function of VWC)	[-]	-1.35
Param2 for CH4 calculations (empirical function of VWC)	[-]	0.20
Param3 for CH4 calculations (empirical function of VWC)	[-]	1.78
Param4 for CH4 calculations (empirical function of VWC)	[-]	6.79
Param1 for CH4 calculations (empirical function of Tsoil)	[-]	0.01
PHENOLOGICAL PARAMETERS		
Length of phenophase (growing degree days). Phase 1	°C	500
Length of phenophase (growing degree days). Phase 2	°C	200
Length of phenophase (growing degree days). Phase 3	°C	500
Length of phenophase (growing degree days). Phase 4	°C	200
Length of phenophase (growing degree days). Phase 5	°C	400
Length of phenophase (growing degree days). Phase 6	°C	200
Length of phenophase (growing degree days). Phase 7	°C	100
Leaf allocation. Phase 1 to phase 7	Ratio	0.40
Fine root allocation. Phase 1 to phase 7	Ratio	0.20
Fruit allocation. Phase 1 to phase 7	Ratio	0.20
Soft stem allocation. Phase 1 to phase 7	Ratio	0.00
Live woody stem allocation. Phase 1 to phase 7	Ratio	0.1
Dead woody stem allocation. Phase 1 to phase 7	Ratio	0.00
Live coarse root allocation. Phase 1 to phase 7	Ratio	0.10
Dead coarse root allocation. Phase 1 to phase 7	Ratio	0.00
Canopy average specific leaf area. Phase 1 to phase 7	$m^2\ kgC^{-1}$	9.81
Current growth proportion. Phase 1 to phase 7	Prop.	0.5

989 **Table A.1** BIOME parameter values after the calibration process.

Parameter	Units	Value
Mineral nitrogen fixed	$kgN\ ha^{-1}\ yr^{-1}$	0
Plant death constant	$gC\ m^{-2}\ d^{-1}$	0.31
Plant residue input C/N ratio	[-]	21.60
Biomass and humus C/N ratio	[-]	14
Synthesis efficiency factor	[-]	0.20
Humification factor	[-]	0.55
Residue mineralization rate (layers 1-3)	day^{-1}	1.39e-3
Humus mineralization rate (layers 1-3)	day^{-1}	4.52e-6
Manure mineralization rate (layers 1-3)	day^{-1}	0.00

NH_4^+ distribution coefficient	$dm^3\ kg^{-1}$	6.85
Molecular diffusion coefficient	$mm^2\ day^{-1}$	120
Volatilization rate	day^{-1}	0.24
Nitrification rate (layers 1-3)	day^{-1}	7.14e-2
Denitrification rate (layers 1-3)	day^{-1}	0.57
Plant nitrogen potential uptake	$kgN\ ha^{-1}\ yr^{-1}$	61.84
Base temperature	°C	20
Q_{10}	[-]	2.22
High end of optimum water content range	[-]	0.08
Lower end of optimum water content	kPa	-162.23
Minimum matric potential for transformation	kPa	-1000
Relative transformation rate at saturation	day^{-1}	0.6
Urea hydrolysis	day^{-1}	0.00
Denitrification half-saturation constant	$mg\ l^{-1}$	10
Limiting NO_3/NH_4 ratio in solution for nitrification	[-]	7.40

990 **Table A.2** LEACHM parameter values after the calibration process.

991

Parameter	Units	Value
Plant death constant	$gC\ m^{-2}\ d^{-1}$	0.72
Plant residue input C/N ratio	[-]	28.94
Humus C/N ratio	[-]	20
Biomass C/N ratio	[-]	8
Respiration rate	[-]	0.6
Humification factor	[-]	0.25
Litter decomposition rate	$m^3\ d^{-1}\ gC^{-1}$	8.00e-6
Humus decomposition rate	$m^3\ d^{-1}\ gC^{-1}$	3.55e-7
Microbial biomass death rate	day^{-1}	2.64e-3
NH_4^+ distribution coefficient	$dm^3\ kg^{-1}$	8.89
Volatilization rate	day^{-1}	1.29e-2
Nitrification rate	$m^3\ d^{-1}\ gC^{-1}$	2.78e-2
Denitrification rate	day^{-1}	3.84e-2
Plant nitrogen potential uptake	$kgN\ ha^{-1}\ yr^{-1}$	118.82
Diffusion coefficient	$m\ d^{-1}$	0.33
Soil moisture threshold for soil water content correction function	$cm\ cm^{-1}$	0.19
Maximum temperature difference	°C	1.16
Optimum temperature	°C	30
Minimum temperature	°C	-5

992 **Table A.3** TETIS-CN parameter values after the calibration process.